Title: Fossils indicate marine dispersal in osteoglossid fishes, a classic example of continental vicariance

Abstract

The separation of closely-related terrestrial or freshwater species by vast marine barriers represents a biogeographic riddle. Such cases can provide evidence for vicariance, a process whereby ancient geological events like continental rifting divided ancestral geographic ranges. With an evolutionary history extending tens of millions of years, freshwater ecology, and distribution encompassing widely separated southern landmasses, osteoglossid bonytongue fishes are a textbook case of vicariance attributed to Mesozoic fragmentation of the Gondwanan supercontinent. Largely overlooked fossils complicate the clean narrative invoked for extant species by recording occurrences on additional continents and in marine settings. Here we present a new total-evidence hypothesis for bonytongue fishes combined with quantitative models of range evolution and show that the last common ancestor of extant osteoglossids was likely marine, and that the group colonized freshwater settings at least four times when both extant and extinct lineages are considered. The correspondence between extant osteoglossid relationships and patterns of continental fragmentation therefore represents a striking example of biogeographic pseudocongruence. Contrary to arguments against vicariance hypotheses that rely only on temporal or phylogenetic evidence, these results provide direct palaeontological support for enhanced dispersal ability early in the history of a group with widely separated distributions in the modern day.

1. Introduction

Why closely related terrestrial and freshwater organisms can be found in landmasses separated by vast stretches of sea is an outstanding question that traces back to the very beginnings of evolutionary biology as a discipline [1,2]. Proposed models to explain these disjunct geographic distributions fall into two broad categories: vicariance, whereby ancient geologic events such as continental breakup created marine barriers and divided ancestral geographic ranges, and long-distance dispersal, whereby organisms dispersed over those barriers more recently. While vicariance became the dominant framework to interpret inter-continental

distributions after the wide acceptance of plate tectonics [3], the last 20 years have seen a resurgence of longdistance dispersal as a plausible and even widespread biogeographic process [4,5]. However, a long-distance dispersal framework has been criticized in the past for relying on *ad hoc* explanations and negative evidence, and for not proposing testable hypotheses [6–8]. Even though most of these critiques have been countered thanks to methodological and statistical advances [5,9], the mechanisms by which terrestrial and freshwater taxa managed to cross oceanic barriers remain unclear, with positive evidence for transoceanic dispersals proving particularly elusive. Further complications emerge when considering the fossil record of extant taxa, as extinct relatives of living organisms can often be found in geographic areas outside their present distribution. Some notable cases include marsupials [10], lungfishes [11], and gars [12], all of which show more complex past geographic distributions. Because of such patterns, the importance of fossils for biogeographic studies has been appreciated for more than a century [2]. Nevertheless, inclusion of fossil data in model-based biogeographic analyses of extant taxa remains limited to just a few remarkable examples in the literature [12–21].

Freshwater fishes in particular provide a model system in historical biogeography due to how evolving geomorphological and tectonic features can present either hard barriers or favorable corridors to their dispersal (e.g., [22–24]). Inclusion of fossils in freshwater fish biogeography is limited by the geographic and temporal patchiness of freshwater deposits with the potential for exceptional preservation of relatively small, delicate vertebrates. Osteoglossomorphs or bonytongue fishes (Osteoglossomorpha) are a celebrated example of a freshwater fish clade with an unusually good fossil record, encompassing every continent except Antarctica and extending to the Late Jurassic–Early Cretaceous (~160–100 Ma) [25,26]. Due to the wide distribution and exclusively freshwater ecology of extant osteoglossomorphs, they have been often viewed as a textbook example of vicariance, either at the level of the entire clade or of some of their subclades, including Osteoglossidae [7,27–29]. Osteoglossidae is today represented by four genera living in South America, Africa, Southeast Asia and Australia. These fishes, commonly called arapaimas and arowanas, include some of the largest freshwater fishes in the world and popular staples of public aquariums for their charismatic and 'prehistoric' appearance. Remarkably, fossils of osteoglossids are found not only outside their current geographic range, but also outside their present environmental tolerance, with several

extinct species known from marine deposits dating to the early Cenozoic (66–40 Ma) (figure 1) [25,26,30,31]. Thus, marine long-distance dispersal represents a possible explanation for the modern disjunct distribution of osteoglossid bonytongues [25,26,30–36], but this hypothesis has never been tested within a phylogenetic framework under a biogeographic model.

Here we estimate ancestral geographic ranges and ancestral habitats for bonytongue fishes under a new total-evidence phylogenetic hypothesis including all extant genera and 32 extinct species of bonytongues. We aim to answer three key questions about the evolutionary history of bonytongue fishes: 1) what are the phylogenetic relationships of extinct marine bonytongues; 2) what are the major patterns of historical biogeography within the clade, and are they consistent with a vicariance or long-distance dispersal framework; 3) are extant freshwater osteoglossids (arapaimas and arowanas) descended from marine ancestors? By doing so, we provide an unprecedented example of how fossil data can dramatically revise biogeographic scenarios that would be strongly supported by the examination of extant species only.

2. Methods

(a) Morphological dataset

The morphological matrix used for the total-evidence phylogenetic analysis of this study is a modification of the morphological dataset of [31], with the novel addition of two extant and 14 extinct species. The list of newly added taxa, complete with the list of specimens and literature used to determine the scoring of morphological characters, is available in the electronic supplementary material. To make the morphological matrix compatible with the molecular dataset for a total-evidence analysis, the taxonomic resolution of extant OTUs (Operational Taxonomic Units) was changed from genus-level to species-level. In the cases where an extant genus was represented by multiple species in the molecular dataset, we assigned the morphological character scoring for that genus to the species that was examined by the original scorer of those characters (e.g., [37]) and/or to the species that we could examine through osteological specimens or μ CT data. Thus, we changed OTUs from the matrix in [31] as follows: $Campylomormyrus \rightarrow C$. $Campylomormyrus \rightarrow C$. Campylomormyru

jardinii. Notably, the morphological characters of this matrix are mostly invariant for congeneric extant species (with the exception of *Scleropages*; see electronic supplementary material), because they were defined to capture morphological variation across Osteoglossomorpha with the purpose of resolving relationships between major bonytongue clades [31,37,38]. The morphological matrix, which ultimately comprised 96 characters for 53 OTUs (33 extinct and 20 extant), was assembled and edited in Mesquite v. 3.61 [39].

(b) Molecular dataset

The molecular data matrix was assembled by integrating part of the genomic dataset of [36] with semi-automated extraction of DNA sequences from Genbank (via the NCBI platform) and BOLD (Barcode Of Life Data system), using functions from the R package regPhylo [40]. A total of 12 DNA markers were selected: two protein-coding mitochondrial markers (col, cytb), two non-protein-coding mitochondrial markers (12S rRNA, 16S rRNA), and eight protein-coding nuclear markers (rag1, rag2, glyt, ficd, megf8, pdzd8, suox, vcpip1). Details of the assemblage of the molecular dataset are available in the electronic supplementary material. As the phylogeny and biogeography of the hyperdiverse Mormyridae (elephantfishes) is not the main focus of this study, we subsampled mormyrids to maximize phylogenetic coverage of the clade while reducing computational burden. The final molecular dataset comprised 14,084 nucleotides for 63 OTUs—including all extant osteoglossomorph genera and 23.4% of all extant osteoglossomorph species—with 87% matrix completeness at the marker level.

(c) Total-evidence phylogenetic analysis

We combined the morphological and molecular matrices to generate a total-evidence dataset including 96 OTUs (33 extinct and 63 extant). A partitioning scheme for the molecular portion of the dataset was determined using PartitionFinder 2 [41], with greedy search algorithm and allowing for partitions based on codon position in the 10 protein-coding markers. As a result, the best partitioning scheme included 8 molecular partitions (electronic supplementary material). The morphological portion of the dataset was treated as a separate additional partition.

An unrooted, non-time-calibrated tree was first estimated in the software MrBayes [42] to provide a starting tree for the time-calibrated phylogenetic analysis (electronic supplementary material, figure S1). *Amia calva* was constrained as the outgroup to all other OTUs, while the other three outgroups (*E. saurus*, *D. cepedianum*, and †Ellimmichthyiformes) were constrained to be outside of total-group Osteoglossomorpha, which included the remaining 93 OTUs. A GTR + Γ + I substitution model was applied to each molecular partition, while an Mk ν substitution model was applied to the morphological partition. The Metropolis-coupled Markov chain Monte Carlo (MCMCMC) was set up as 2 runs with 4 chains each, running for 50 million generations and sampling every 10,000. Parameter summaries and the 'Allcompat' summary consensus tree were calculated using a 50% burn-in fraction.

107

108

109

110

111

112

113

114

115

116

117

118

119

120

121

122

123

124

125

126

127

128

129

130

131

132

133

After the unrooted analysis, we ran a Bayesian time-calibrated phylogenetic analysis in MrBayes under a Skyline Fossilized Birth Death model (SFBD) [43]. The analysis was run on the PalMuc High-Performance Computing (HPC) cluster at LMU Munich. As in the unrooted analysis, a GTR + Γ + I substitution model was applied to each molecular partition and an Mkv substitution model was applied to the morphological partition, with all characters unordered. A relaxed clock model with independent gamma rates (IGR) was applied separately to the mitochondrial, nuclear, and morphological portions of the dataset, to allow for rate variation across branches. The prior on the average clock rate was set as a lognormal distribution with mean equal to -5.3 (5*10⁻³ on a real scale, corresponding to the unrooted tree height divided by the minimum age of the tree in Ma as set by the tree age prior) and standard deviation equal to 1.17481 (corresponding to two orders of magnitude for a lognormal distribution). The prior on the clock rate variance was set as an exponential distribution with mean equal to 0.587405, corresponding to approximately one order of magnitude of clock rate variance across branches. The SFBD tree model was set up to allow fossil sampling rate to vary between four time intervals: pre-Cretaceous (up to 145 Ma), Cretaceous (145–66 Ma), Paleocene-Eocene (66-33.9 Ma), Oligocene-Recent (33.9-0 Ma). The time intervals were chosen based on a priori knowledge of the bonytongue fossil record: no articulated bonytongue fossil has ever been found in deposits older than the Cretaceous, despite evidence of a much earlier origin [26]; and definitive fossils of the group are found in marine deposits only in the Paleocene-Eocene interval [30]. We did not allow extinct taxa to be recovered as sampled ancestors, as incorrectly recovered sampled ancestors (false positives) might

heavily bias downstream ancestral state reconstructions like the biogeographic analyses performed in this study, due to their zero-length branches. The sampling probability for extant tips was fixed to 0.234, corresponding to the fraction of extant osteoglossomorph species included in the analysis [44]. In addition to the topological constraints used in the unrooted analysis, two large clades were constrained as monophyletic to ease convergence of the time-calibrated analysis: total-group Osteoglossidae (0.97 posterior probability in the unrooted phylogeny), and total-group Notopteroidea (0.85 posterior probability in the unrooted phylogeny). The monophyletic constraint on total-group Notopteroidea was necessary to set †Palaeonotopterus within this clade. This position is strongly supported by osteological studies [45] and by non-time-calibrated phylogenetic analyses [31,37,38,this study]. However, preliminary FBD tip-dating analyses without the Notopteroidea constraint showed a highly unstable position of †*Palaeonotopterus*, likely due to the combination of very old age (early Cenomanian) and few morphological characters (23 out of 96 total) scored for this taxon. A redescription of †Palaeonotopterus including recently found, more complete material (L. Cavin, pers. comm.) and revised character scoring might help stabilize the phylogenetic position of this taxon for future studies. Tip ages of extinct taxa were assigned a prior uniform distribution ranging from minimum to maximum possible age of the fossil deposit where that taxon has been found. A list of all fossil tip ages with references can be found in the electronic supplementary material. Moreover, a node age calibration was applied to total-group Osteoglossomorpha (offset lognormal distribution with minimum = 130 Ma, soft 95% probability density maximum = 206.9 Ma, standard deviation = 19.75 Ma), with minimum age older than the oldest extinct osteoglossomorphs included in this analysis (†Asiatolepis and †Lycoptera), and soft maximum based on the maximum origin age estimate of [26]. The tree age prior was set up to match a likely origin age for crown Neopterygii (offset lognormal distribution with minimum = 251.9 Ma, mean = 280 Ma, standard deviation = 23.59 Ma), with minimum age based on the oldest unquestionable fossil of a crown neopterygian (the halecomorph †Watsonolus [46]), and mean age based on the mean age estimate of [47]. The MCMCMC was set up as 2 runs with 4 chains each, running for 450 million generations and sampling every 1,000, with 10% burn-in fraction. Convergence of parameters between the two runs was checked in Tracer [48] by comparing their posterior estimates and by calculating their Effective Sample Sizes (ESSs), which were >200 for all parameters. Posterior tree files were resampled as one tree every 10,000

134

135

136

137

138

139

140

141

142

143

144

145

146

147

148

149

150

151

152

153

154

155

156

157

158

159

generations before calculating the 'Allcompat' summary consensus tree (a majority rule tree showing all compatible taxon bipartitions). The phylogenetic position of extinct taxa in respect to extant ones across the posterior distribution of trees was evaluated using the function 'create.rogue.plot' from the R script RoguePlots [49].

(d) Biogeographic analysis

The biogeographic analysis was set up and run in the R package Biogeobeans [50]. Continental land masses were divided into 7 areas encompassing the whole distribution of extant and extinct Osteoglossomorpha and corresponding to major biogeographical regions for extant freshwater fishes [22]: Nearctic, Neotropical, Ethiopian, Palearctic, Sinean, Indo-Malayan (or Oriental), and Australian. For simplicity, we refer to these regions respectively as North America, South America, Africa, Europe, continental Asia, Indo-Malaya, and Australia in the main text and figures. Additionally, we considered the marine realm as an additional geographic area (bringing the total to 8 areas), and extinct taxa found in marine deposits were scored as occurring exclusively in the marine area.

We also tested an alternative scoring scheme where extinct taxa found in marine deposits were scored as belonging to the continental biogeographic regions where their fossils have been found in (electronic supplementary material). This alternative scoring scheme, while providing more granular information about the geographic distribution of marine bonytongues, has the disadvantage of confounding marine and freshwater biogeographic regions (e.g., a marine taxon found in North America could come from the eastern Pacific or the western Atlantic, two very distinct regions with different biogeographic affinities). Thus, we will primarily refer to results obtained under the first scoring scheme.

The maximum number of areas that could be occupied by a single lineage at any one point was fixed to 3, to reduce the number of allowed geographic states and reduce computational time. We further restricted the state space of the analysis by removing all geographic states corresponding to the marine realm plus two continental regions, but we kept states corresponding to the marine realm plus one continental region to potentially allow for a euryhaline (freshwater + marine) condition.

We applied the standard biogeographic models implemented in Biogeobears on the 'AllCompat' summary consensus tree obtained by the total-evidence phylogenetic analysis. These models include DEC (Dispersal-Extinction-Cladogenesis [51]), DIVALIKE (a likelihood interpretation of the parsimony DIVA, DIspersal Vicariance Analysis model [52]), and BAYAREALIKE (a simplified likelihood interpretation of the Bayesian model implemented in the software 'BayArea' [53]). Additionally, we ran variants of these three models that include a jump dispersal parameter, *j*, which allows for founder-event jump dispersal during cladogenesis (see [54] for a critique of the DEC+*j* model, and [55] for a partial response to that critique). Standard tools for statistical model comparison [56] – including likelihood ratio test for pairs of nested models and Akaike Information Criterion for small sample sizes (AICc) – were used to evaluate model support.

To test how phylogenetic uncertainty impacts the results of the biogeographic analysis, we applied the best-fitting biogeographic model to 200 phylogenies sampled from the Bayesian posterior distribution. The results from these 200 analyses were summarized by recording marginal ancestral area reconstructions for 8 clades: total-group Osteoglossomorpha (root node), crown Osteoglossomorpha (*Hiodon alosoides* + *Osteoglossum bicirrhosum* node), crown Osteoglossiformes (*Pantodon buccholzi* + *Osteoglossum bicirrhosum* node), crown Osteoglossidae (*Osteoglossum bicirrhosum* + *Arapaima gigas* node), crown Osteoglossinae (*Osteoglossum bicirrhosum* + *Scleropages formosus* node), crown Arapaiminae (*Arapaima gigas* + *Heterotis niloticus* node), crown Notopteroidei (*Notopterus notopterus* + *Mormyrus ovis* node), and crown Notopteridae (*Notopterus notopterus* + *Papyrocranus afer* node). For these clades, we calculated average marginal probabilities for each possible state, corresponding to empirical Bayesian posterior probabilities.

To explore how the inclusion of fossil data impacts biogeographic inference, we ran the standard BioGeoBEARS models listed above on the Bayesian consensus tree pruned of all extinct taxa. We compared marginal ancestral states found in this extant-only analysis with marginal ancestral states recovered from the previous integration of 200 phylogenies with extinct taxa from the posterior distribution.

To examine dispersal directionality between the 8 biogeographical regions, we performed biogeographical stochastic mapping (BSM) [57] as implemented in BioGeoBEARS. We simulated 100 BSMs under the best-fitting parameters with the DEC+*j* model for each of the 200 phylogenies previously

sampled from the Bayesian posterior distribution. The average number of dispersal events from and to each biogeographical region, comprehensive of both anagenetic and cladogenetic ("jump") dispersal, were tabulated for each of the 200 posterior phylogenies, and then averaged across phylogenetic uncertainty by calculating their mean.

(e) Ancestral habitat estimation

As a complementary approach to reconstruct transitions between freshwater regions and the marine realm, we applied ancestral state estimation (ASE) on a binary ecological character (freshwater vs marine) in the R package corhmm [58]. Extinct taxa were assigned to the freshwater or marine state depending on the paleoenvironmental reconstruction of the fossil deposits they have been found in (electronic supplementary material). We estimated marginal ancestral states under an all-rates-different (ARD) model on the Bayesian consensus tree, with root state probabilities based on the estimated transition rates (root.p="yang" flag in the corhmm function). To estimate the number of transition events from freshwater to marine environments and vice versa, we used the makeSimmap function to generate 10000 stochastic character mappings on the Bayesian consensus tree using the maximum likelihood transition rate matrix previously calculated under the ARD model.

In order to account for phylogenetic uncertainty when estimating freshwater-marine transitions, stochastic character mapping was also performed on a random sample of 1000 phylogenies from the Bayesian posterior distribution in the R package phytools [59]. Ten stochastic character mappings were generated for each sampled phylogeny under the ARD model with estimated root state probabilities. The simulated number of transition events from freshwater to marine environments and vice versa were summarized by plotting histograms and by calculating mean and relevant quantiles.

3. Results

(a) Phylogenetic relationships

Most major phylogenetic relationships recovered in the Bayesian total-evidence time-calibrated phylogenetic analysis (figure 2) are compatible with previous morphological and molecular studies (e.g.,

[36–38,60–63]; see [25] for a review of osteoglossomorph systematics). These include mooneyes (Hiodontidae) as living sister group to all other extant bonytongues (Osteoglossiformes); elephantfishes (Mormyridae) and the aba (Gymnarchidae) as closely related to Old World knifefishes (Notopteridae); and arapaimas and relatives (Arapaiminae) being closely related to arowanas (Osteoglossinae) and forming the clade Osteoglossidae. The African butterflyfish *Pantodon* was recovered as living sister group to all other extant Osteoglossiformes, a position that is not supported by morphological characters alone [31,37,38] but which is often found in molecular phylogenetic analyses (e.g., [36,63]). Intergeneric relationships within the species-rich Mormyridae match those recovered by [36].

The posterior probabilities of several nodes forming the 'backbone' of the osteoglossomorph tree are extremely low due to the uncertain position of several extinct taxa (figure 2). However, even when posterior probabilities of nodes including extinct taxa are very low, those taxa might consistently resolve in few distinct positions compared to extant taxa [49]. Hence, exploring the position of extinct taxa in respect to extant ones across the posterior distribution of phylogenies can be more informative than just examining node supports on a consensus tree (electronic supplementary material, figure S2). Relationships of non-osteoglossid extinct taxa broadly match previous hypotheses, and are discussed in further detail in the electronic supplementary material.

All marine taxa included in the analysis (†Brychaetus, †Furichthys, †Heterosteoglossum, †Macroprosopon, †Magnigena, †Thrissopterus, †Xosteoglossid and the undescribed Habib Rahi taxon) are recovered as either crown or stem members of Osteoglossidae. Some of them are often grouped together with extinct freshwater taxa from various continents (†Phareodus, †Phareoides, †Taverneichthys and †Cretophareodus), making up the clade †Phareodontinae (sensu [31]). The position of †Phareodontinae within Osteoglossidae is not well resolved, although a stem osteoglossid position is more favored than other placements. The marine taxa †Heterosteoglossum and †Thrissopterus are most often recovered as stem members of Arapaiminae. †Sinoglossus from the late Eocene–Oligocene (~38–23 Ma) of China is either reconstructed as sister to the African Heterotis, or as sister to the South American Arapaima. The Eocene

Chinese species of *Scleropages* ($\dagger S$. *sinensis* and $\dagger S$. *sanshuiensis*) resolve almost always as stem Osteoglossinae, suggesting they might represent members of an extinct genus distinct from *Scleropages*.

(b) Evolutionary timescale

Our Bayesian time-calibrated phylogenetic analysis provides the most comprehensive assessment of the evolutionary timescale of bonytongue fishes to date. Osteoglossomorph origin is estimated to occur between the Late Triassic and the Early Jurassic (95% highest posterior density (HPD) = 235.3–175.3 Ma). This is older than previous fossil-based estimates [26], but slightly younger than estimates based only on molecular data [36,61,64]. Crown Osteoglossiformes appear to have originated in the Jurassic (95% HPD = 196.8–145.4 Ma), while the divergence between the two largest bonytongue clades (Osteoglossidae on one side, Mormyroidei and Notopteridae on the other) occurred between the Middle Jurassic and the very beginning of the Early Cretaceous (95% HPD = 173.1–131.4 Ma). Old World knifefishes (Notopteridae) diverged from elephantfishes and relatives (Mormyroidei) in the Early Cretaceous (95% HPD = 137.5–107.3 Ma). The divergence between extant African and Asian knifefishes likely happened in the Late Cretaceous (95% HPD = 104.3–60.6 Ma), significantly postdating the fragmentation of East and West Gondwana [35]. The hyper-diverse elephantfishes started diversifying between the Paleocene and the early middle Eocene (95% HPD = 64.7–40.9 Ma), with most divergences between extant genera occurring in the Oligocene and Miocene.

The origin of osteoglossid bonytongues is estimated to occur between the Early Cretaceous and the early Late Cretaceous (95% HPD = 137.7–89.7 Ma). The divergence between Arapaiminae and Osteoglossinae (crown Osteoglossidae) likely happened in the Late Cretaceous before the Maastrichtian (95% HPD = 108.9–72.5 Ma). The split between the South American *Arapaima* and the African *Heterotis* likely occurred between the Maastrichtian and the middle Eocene (95% HPD = 70.4–37.5 Ma), while the split between the Southeast Asian *Scleropages formosus* and the South American *Osteoglossum* is estimated to occur in the Paleocene–Eocene interval (95% HPD = 64.5–31.3 Ma). These divergences between osteoglossid genera inhabiting disjunct continents postdate the fragmentation of Gondwanan landmasses,

except for the separation between South America, Antarctica and Australia, which likely occurred during the Paleocene–Eocene interval [65].

(c) Historical biogeography and freshwater-marine transitions

In a biogeographic analysis excluding fossils, we find a pattern broadly consistent with a continental vicariance scenario that matches previous hypotheses for the biogeographic history of bonytongues [7,27–29]. Major biogeographic findings include a West Gondwanan plus North American ancestral distribution for crown osteoglossomorphs, and a West Gondwanan ancestral distribution for crown osteoglossids (figure 3a; electronic supplementary material, figures S3 and S4). Both are associated with major vicariant splits: the split between Laurasia and Gondwana leads to the North American *Hiodon* on one side and to the Gondwanan Osteoglossiformes on the other, while the split between Africa and South America leads to *Heterotis* on one side and to South American osteoglossids on the other.

Fossils radically revise this picture of osteoglossomorph biogeography. Our two approaches to considering marine associations in extinct osteoglossomorphs yield consistent and complementary inferences about the group's biogeographical and ecological history. When marine settings are treated as a biogeographic region, we find a marine ancestral distribution for crown osteoglossids under the DEC+*j* model (figure 2). This striking result is robust to phylogenetic uncertainty (figure 3*a*). The ancestral distributions of both crown Osteoglossinae and crown Arapaiminae are not reconstructed as marine and are instead uncertain between the freshwater geographic areas in which their members are found (Indo-Malaya, Australia and South America for crown Osteoglossinae; Africa, continental Asia and South America for crown Arapaiminae). However, this might represent a conservative result due to the likely under-parameterized nature of the biogeographic models used here (see Discussion). Other key biogeographic findings include a Laurasian (Asia + North America) origin for crown osteoglossomorphs, followed by a dispersal from Laurasian landmasses to Africa leading to the origin of Osteoglossiformes. The specific source of this

dispersal (North America or Asia) is sensitive to topological differences in the posterior distribution of phylogenies.

When marine and freshwater settings are treated as a binary ecological character evolving under an all-rates-different (ARD) Markov model, we also find strong support for an ancestral marine ecology in crown osteoglossids (figure 4). Rates of transition between marine and freshwater environments are strongly asymmetric, with the marine-to-freshwater transition rate estimated to be more than one order of magnitude larger than the freshwater-to-marine rate (freshwater-to-marine rate = $7.47*10^{-4}$ Myr⁻¹ per lineage; marine-to-freshwater rate = $1.96*10^{-2}$ Myr⁻¹ per lineage). This asymmetry is reflected in the number of transitions calculated across 1000 stochastic character mappings simulated under maximum likelihood parameter estimates on the Bayesian consensus tree (figure 4c). Bonytongue fishes invaded marine environments on average 1.9 times (mode = 1, corresponding to the marine invasion associated with the origin of the osteoglossid lineage), but they reentered freshwater environments on average 6.3 times (mode = 5). Comparable results are found when considering phylogenetic uncertainty by simulating stochastic character mappings across a sample of the Bayesian posterior distribution of trees (electronic supplementary material, figure 85).

4. Discussion

(a) Biogeographic history of Osteoglossomorpha

A comprehensive picture of the biogeographic history of Osteoglossomorpha can be reconstructed by integrating the divergence-time estimates and ancestral eco-geographical reconstructions obtained in this study with Earth's geo-palaeontological history. The ancestral osteoglossomorph likely lived in freshwater environments in the Laurasian supercontinent between the Late Triassic and Early Jurassic. Several early-diverging lineages of osteoglossomorphs are found both in Asian and North American fossil deposits, hinting at multiple dispersals between these continents during the Mesozoic. Faunal exchanges between Asia and North America in the Jurassic and Cretaceous are strongly supported for several groups of continental organisms, including dinosaurs, mammals, and several other freshwater fish taxa [26,66]. Crown Osteoglossiformes are here inferred to have an African origin in the Jurassic. Strikingly, while no articulated

bonytongue fossil has ever been found in African Jurassic deposits, fragments of scales (squamules) similar to those of modern osteoglossiforms have been recovered from the Middle Jurassic Anoual Formation of Morocco [67], matching our age estimate for the origin of Osteoglossiformes and providing a potential earliest occurrence of this group in the African continent. Moreover, a dispersal from North America to Africa—potentially via Europe—in the Jurassic would be consistent with the similarities among Late Jurassic terrestrial faunas of these continents [66,68]. Given the long evolutionary history of osteoglossiforms in Africa, it is perhaps surprising that fossils of these fishes are almost absent from South American Mesozoic deposits, as South America and Africa were joined into a single continental landmass until the beginning of the Late Cretaceous, around 100 Ma [69]. The only exception is represented by †*Laeliichthys*, a close South American relative of notopterid knifefishes, a clade that today inhabits only Africa and southeast Asia. Crown notopterids are reconstructed as ancestrally African like other osteoglossiforms, and they probably dispersed from Africa to the Indian subcontinent in the Late Cretaceous across a narrow Mozambique Channel [25,26].

The last common ancestor of all osteoglossids (extant and extinct) included in this analysis is inferred to have been marine, probably descending from an African freshwater lineage of osteoglossiforms (with some uncertainty between African and North American origin under the alternative biogeographic scoring scheme; see electronic supplementary material). All three major clades within Osteoglossidae (†Phareodontinae, Arapaiminae and Osteoglossinae) have likely originated from marine ancestors, and reinvaded freshwater habitats multiple times independently in different continents—including North America, Asia, Australia and South America. Though starkly in contrast with traditional views of bonytongue biogeography (e.g., [7]), these results strongly support recent hypotheses of marine dispersal as the biogeographic process responsible for the disjunct distribution of extant osteoglossid bonytongues [30,35,36]. The four-to-five independent transitions towards freshwater environments from the marine realm reconstructed from biogeographic stochastic mappings (figure 3b–c) are very likely to be an underestimate. This is due to the somewhat simplistic nature of the DEC+j model used for the biogeographic analysis, which assumes that the per-lineage dispersal rates between regions are all equal, symmetric, and constant through time, and does not penalize direct dispersal between very distant freshwater regions. For example, the two closely related Eocene freshwater genera †Phareodus and †Phareoides are respectively from the western

United States and from Australia, and our analysis reconstructs their ancestral geographic area to be either North America or Oceania, implying a direct long-distance dispersal from one to the other without passing through a marine stage. Given that these genera are nested within a marine clade (figure 2), it is not unreasonable to hypothesize that they might instead represent two independent freshwater invasions from marine ancestors, not captured by the DEC+*j* model. A similar reasoning might be applied to the reconstructed ancestral areas of crown Osteoglossinae and crown Arapaiminae (see Results). Thus, we predict that biogeographic models downweighting direct dispersal between distant freshwater regions would recover an even more preeminent role of marine dispersal and marine-to-freshwater transitions in the biogeographic history of bonytongue fishes.

(b) Marine origin and dispersal in bonytongue fishes

Speculation on marine dispersal in osteoglossid bonytongues began with recognition of the Eocene †Brychaetus as an osteoglossid [32]. Several more taxa have been subsequently described from marine deposits, all restricted to the early Palaeogene [33,34,70]. However, the lack of a phylogenetic framework and the uncertain systematics of these marine forms hindered any formal test of the marine dispersal hypothesis. Until now, the strongest arguments in favor of marine dispersal in osteoglossids came from estimated divergence times younger than the continental fragmentation of Gondwana [35,36,71], and from the observation that closely related Palaeogene taxa—sometimes even classified in the same genus—have been found in freshwater deposits as distant as Wyoming is from Australia [30]. Here we provide direct fossil evidence for marine dispersal in the lineage leading to extant osteoglossid bonytongues—arowanas and arapaimas. We find that, rather than forming a single clade or being randomly interspersed across bonytongue phylogeny, marine bonytongues form a 'cloud' at the base of Osteoglossidae from which all three major osteoglossid subclades (Arapaiminae, Osteoglossinae and †Phareodontinae) emerged. Ancestral state reconstructions strongly support a single freshwater-to-marine transition on the osteoglossid stem, followed by at least four—but likely more—independent marine-to-freshwater reversals. This result is remarkable for several reasons. Firstly, to our knowledge, this is the first time that a group (crown Osteoglossidae) whose extant members and closer extant relatives are all exclusively freshwater is reconstructed as ancestrally marine. Secondly, major environmental transitions such as the freshwater-to-marine one are rare—albeit not unlikely—in teleost fish groups [72,73]. Lastly, this reconstruction implies that several distinct lineages of osteoglossids were wiped out from marine environments around or soon after the middle Eocene, and that these fishes never reinvaded the sea afterwards. More palaeontological data would be needed to test whether competition with other predatory fishes such as several acanthomorph lineages who diversified around the same time [74], or severe climate change towards colder temperatures in the middle Eocene–Oligocene interval [75] played some role in the demise of marine bonytongues.

397

398

399

400

401

402

403

404

405

406

407

408

409

410

411

412

413

414

415

416

417

418

419

420

421

422

423

Because occurrences of bonytongue fossils in marine deposits are mostly restricted to the early Palaeogene (figure 1), it has been previously suggested that the evolution of marine bonytongues might have happened on the wake of the Cretaceous-Palaeogene (K-Pg) mass extinction that wiped out several large predators [76], and triggered the diversification of new clades, including most modern lineages of marine piscivorous fishes [29,77]. However, our total-evidence analysis recovers a much older origin of marine bonytongues, with the ancestral osteoglossid—reconstructed as marine—originating deep in the Cretaceous, at least 90 million years ago (figure 2). Several factors—not mutually exclusive—might explain this 25 Myr discrepancy between the oldest known marine bonytongue fossils and the youngest inferred age for the ancestral osteoglossid. It is possible that bonytongues invaded marine environments early in the Cretaceous, but remained geographically and/or ecologically restricted for several million years, until the K-Pg mass extinction. If that was the case, then their absence from the Cretaceous marine fossil record could be more easily explained by regional (rather than global) patterns of the marine fossil record. Our results suggest that the bonytongue lineage leading to osteoglossids and to the freshwater-to-marine transition was likely African (although this is more uncertain under our alternative biogeographic scoring scheme; see electronic supplementary material), and the marine fossil fish record of the Late Cretaceous of Africa is extremely limited—virtually non-existent in sub-Saharan Africa [78]. Another possible explanation for the age discrepancy pertains to the tree model employed for our total-evidence phylogenetic analysis, which assumes constant diversification rates through time and among lineages. If the environmental transition at the base of Osteoglossidae triggered an increase in the diversification rate of the group compared to other bonytongues, then a constant diversification model would likely overestimate the origin age of osteoglossids.

(c) Impact of fossil data on biogeographic inference

Bonytongue fishes represent a striking case study of how the inclusion of fossil data can dramatically alter biogeographic inference for extant organisms. Such an outcome might happen for two main reasons: 1) extinct taxa might be found in geographic areas outside the modern biogeographic range of the clade of interest; 2) extinct taxa might display eco-morphological characteristics that are outside the spectrum of adaptations found in extant representatives of the same clade. In the case of bonytongue fishes, both reasons apply: extinct bonytongues have been found in Europe and continental Asia, where they are completely absent today; and bonytongue fossils have been found in marine deposits, demonstrating a much broader ecological tolerance in the past than today. The fossil record has arguably caught osteoglossid bonytongues in the act, providing us with a snapshot of their marine-adapted evolutionary history which would have otherwise remained concealed. Face-value interpretation of biogeographic patterns derived exclusively from modern distributions can lead to a partial—if not outright wrong—inference by ignoring a key data source like the fossil record, as showcased by the results of our biogeographic analysis when excluding extinct taxa (figure 3*a*; electronic supplementary material, figures S3 and S4).

Despite the obvious relevance of fossil data, some limitations remain to their inclusion in phylogeny-based biogeographic studies. Firstly, fragmentary fossils are often not included in tip-dating phylogenetic analyses because they cannot be scored for the vast majority of characters in a morphological matrix. However, fragmentary specimens still provide useful biogeographic information if they can be at least assigned to a broad taxonomic level (such as family or order). For example, they can record the first or only occurrence of a clade in a certain geographic area. This information is lost when including only more complete fossils that are diagnostic at species-level into biogeographic analyses. Secondly, current phylogeny-based biogeographic models such as DEC do not take into account spatial and temporal biases of the fossil record [79]. The effect of these biases on biogeographic analyses that include extinct taxa as tips has been explored only in limited cases [80,81] and never for DEC-like models, but it is likely that they have an impact on reconstructed ancestral areas. As biogeographic studies including fossils as sampled tips will

become more common in the future, further exploration of fossil record biases in biogeographic inference will be paramount.

Occurrence-based approaches to biogeographic inference can accommodate both fragmentary fossils and spatio-temporal biases of the fossil record [82,83], but they lack phylogenetic information. Time-stratified, spatially-explicit models of fossil preservation potential could be developed in a Bayesian phylogenetic framework, similarly to how the geographical structure of biomes over time and its interaction with lineage dispersal has been recently modeled [84]. At the same time, fossil occurrence data can be jointly modeled with a phylogenetic tree through the occurrence birth-death process [85], and relevant biogeographic parameters such as dispersal rates might be estimated under this framework. While a comprehensive modeling of spatio-temporal fossilization dynamics for phylogeny-based biogeographic inference will pose several technical and computational challenges, it represents a promising research avenue to properly utilize an invaluable data source that cannot be substituted by neontological data, as demonstrated by the case of bonytongue fishes.

References

- 1. Darwin C., On the Origin of Species by Means of Natural Selection, or the Preservation of Favoured Races in the Struggle for Life (John Murray, London, UK, 1859).
- A. R. Wallace, The geographical distribution of animals; with a study of the relations of living and
 extinct faunas as elucidating the past changes of the Earth's surface (Harper & Brothers, New York,
 NY, 1876).
 - 3. E. O. Wiley, Vicariance biogeography. Ann. Rev. Ecol. Syst. 19, 513–542 (1988).
- 4. A. de Queiroz, The resurrection of oceanic dispersal in historical biogeography. *Trends Ecol. Evol.*20, 68–73 (2005).
- 5. R. G. Gillespie *et al.*, Long-distance dispersal: a framework for hypothesis testing. *Trends Ecol. Evol.* 27, 47–56 (2012).

- 477 6. G. Nelson, D. E. Rosen, Vicariance biogeography: a critique: symposium of the Systematics
- Discussion Group of the American Museum of Natural History, May 2-4, 1979 (Columbia
- 479 University Press, New York, NY, 1981).
- 480 7. G. Nelson, P. Y. Ladiges, Gondwana, vicariance biogeography and the New York School revisited.
- 481 Aust. J. Bot. 49, 389–409 (2001).
- 482 8. J. S. Sparks, W. L. Smith, Freshwater fishes, dispersal ability, and nonevidence: "Gondwana life
- 483 rafts" to the rescue. *Syst. Biol.* **54**, 158–165 (2005).
- 9. M. D. Crisp, S. A. Trewick, L. G. Cook, Hypothesis testing in biogeography. *Trends Ecol. Evol.* **26**,
- 485 66–72 (2011).
- 486 10. J. J. Jaeger, M. Martin, African marsupials—vicariance or dispersion? *Nature* 312, 379 (1984).
- 11. J. A. Clack, E. L. Sharp, J. A. Long, "The fossil record of lungfishes" in *The Biology of Lungfishes*,
- J. M. Jørgensen, J. Joss, Eds. (CRC Press, Boca Raton, 2010), pp. 1–42.
- 489 12. C. D. Brownstein, L. Yang, M. Friedman, T. J. Near, Phylogenomics of the ancient and species-
- depauperate gars tracks 150 million years of continental fragmentation in the northern hemisphere.
- 491 Syst. Biol. 72, 213–227 (2023).
- 492 13. H. M. Wood, N. J. Matzke, R. G. Gillespie, C. E. Griswold, Treating fossils as terminal taxa in
- divergence time estimation reveals ancient vicariance patterns in the palpimanoid spiders. Syst. Biol.
- **62**, 264–284 (2013).
- 495 14. G. S. Ferreira, M. Bronzati, M. C. Langer, J. Sterli, Phylogeny, biogeography and diversification
- patterns of side-necked turtles (Testudines: Pleurodira). R. Soc. Open Sci. 5, 171773 (2018).
- 497 15. L. Varela, P. S. Tambusso, H. G. McDonald, R. A. Fariña, Phylogeny, macroevolutionary trends
- 498 and historical biogeography of sloths: insights from a Bayesian morphological clock analysis. Syst.
- 499 *Biol.* **68**, 204–218 (2019).
- 500 16. G. H. Azevedo et al., Fossils constrain biogeographical history in a clade of flattened spiders with
- transcontinental distribution. J. Biogeogr. 48, 3032–3046 (2021).
- 502 17. Y. Yan *et al.*, Phytogeographic history of the tea family inferred through high-resolution phylogeny
- 503 and fossils. Syst. Biol. 70, 1256–1271 (2021).

- 18. C. D. Bacon, D. Silvestro, C. Hoorn, G. Bogotá-Ángel, A. Antonelli, N. Chazot, The origin of
- modern patterns of continental diversity in Mauritiinae palms: the Neotropical museum and the
- 506 Afrotropical graveyard. *Biol. Lett.* **18**, 20220214 (2022).
- 507 19. A. L. Wisniewski, G. T. Lloyd, G. J. Slater, Extant species fail to estimate ancestral geographical
- ranges at older nodes in primate phylogeny. *Proc. Biol. Sci.* **289**, 20212535 (2022).
- 509 20. Q. Zhang, R. H. Ree, N. Salamin, Y. Xing, D. Silvestro, Fossil-informed models reveal a
- boreotropical origin and divergent evolutionary trajectories in the walnut family (Juglandaceae).
- 511 Syst. Biol. 71, 242–258 (2022).
- 512 21. M. Coiro, R. Allio, N. Mazet, L. J. Seyfullah, F. L. Condamine, Reconciling fossils with phylogenies
- reveals the origin and macroevolutionary processes explaining the global cycad biodiversity. *New*
- 514 *Phytol.* Early View, 1–20. (2023).
- 515 22. B. Leroy et al., Global biogeographical regions of freshwater fish species. J. Biogeogr. 46, 2407–
- **516** 2419 (2019).
- 517 23. P. Val, N. J. Lyons, N. Gasparini, J. K. Willenbring, J. S. Albert, Landscape evolution as a
- 518 diversification driver in freshwater fishes, Front. Ecol. Evol. 9, 788328 (2022).
- 519 24. F. A. Cassemiro et al., Landscape dynamics and diversification of the megadiverse South American
- 520 freshwater fish fauna. *Proc. Natl. Acad. Sci. U.S.A.* **120**, e2211974120 (2023).
- 521 25. E. J. Hilton, S. Lavoué, A review of the systematic biology of fossil and living bonytongue fishes,
- 522 Osteoglossomorpha (Actinopterygii: Teleostei). *Neotrop. Ichthyol.* **16**, e180031 (2018).
- 523 26. A. Capobianco, M. Friedman, Vicariance and dispersal in southern hemisphere freshwater fish
- 524 clades: a palaeontological perspective. *Biol. Rev.* **94**, 662–699 (2019).
- 525 27. J. Cracraft, Continental drift and vertebrate distribution. Ann. Rev. Ecol. Syst. 5, 215–261 (1974).
- 526 28. P. B. Moyle, J. J. Jr. Cech, Fishes. An Introduction to Ichthyology, 4th Edition (Prentice-Hall Inc.,
- 527 Upper Saddle River, NJ, 2000).
- 528 29. M. Barton, Bond's Biology of Fishes, 3rd Edition (Brooks/Cole Publishing Company, Pacific Grove,
- 529 CA, 2006).
- 30. A. Capobianco, E. Foreman, M. Friedman, A Paleocene (Danian) marine osteoglossid (Teleostei,

- Osteoglossomorpha) from the Nuussuaq Basin of Greenland, with a brief review of Palaeogene marine bonytongue fishes. *Pap. Palaeontol.* 7, 625–640 (2021).
- 31. A. Capobianco, S. Zouhri, M. Friedman, A long-snouted marine bonytongue (Teleostei:
- Osteoglossidae) from the early Eocene of Morocco and the phylogenetic affinities of marine
- osteoglossids. Zool. J. Linn. Soc. (in press).
- 536 32. C. Patterson, The distribution of Mesozoic freshwater fishes. *Mem. Mus. Natl. Hist. Nat. Série A*
- 537 *Zoologie* **88**, 156–174 (1975).
- 33. N. Bonde, Osteoglossomorphs of the marine Lower Eocene of Denmark-with remarks on other
- Eocene taxa and their importance for palaeobiogeography. Geol. Soc. Spec. Publ. 295, 253-310
- 540 (2008).
- 541 34. P. L. Forey, E. J. Hilton, "Two new tertiary osteoglossid fishes (Teleostei: Osteoglossomorpha) with
- notes on the history of the family" in Morphology, Phylogeny and Paleobiogeography of Fossil
- Fishes, D. K. Elliott, J. G. Maisey, X. Yu, D. Miao, Eds. (Verlag Dr. F. Pfeil, München, 2010), pp.
- 544 215–246.
- 545 35. S. Lavoué, Was Gondwanan breakup the cause of the intercontinental distribution of
- Osteoglossiformes? A time-calibrated phylogenetic test combining molecular, morphological, and
- paleontological evidence. Mol. Phylogenet. Evol. 99, 34–43 (2016).
- 36. R. D. Peterson et al., Phylogenomics of bony-tongue fishes (Osteoglossomorpha) shed light on the
- craniofacial evolution and biogeography of the weakly electric clade (Mormyridae). Syst. Biol. 71,
- 550 1032–1044 (2022).
- 551 37. E. J. Hilton, Comparative osteology and phylogenetic systematics of fossil and living bony-tongue
- fishes (Actinopterygii, Teleostei, Osteoglossomorpha). Zool. J. Linn. Soc. 137, 1–100 (2003).
- 553 38. M. V. H. Wilson, A. M. Murray, Osteoglossomorpha: phylogeny, biogeography, and fossil record
- and the significance of key African and Chinese fossil taxa. Geol. Soc. Spec. Publ. 295, 185–219
- 555 (2008).
- 556 39. W. P. Maddison, D.R. Maddison, Mesquite: a modular system for evolutionary analysis. Version
- 3.61 (2019). Available at http://www.mesquiteproject.org

- 558 40. D. Eme, M. J. Anderson, C. D. Struthers, C. D. Roberts, L. Liggins, An integrated pathway for
- building regional phylogenies for ecological studies. *Glob. Ecol. Biogeogr.* **28**, 1899–1911 (2019).
- 41. R. Lanfear, P. B. Frandsen, A. M. Wright, T. Senfeld, B. Calcott, PartitionFinder 2: new methods
- for selecting partitioned models of evolution for molecular and morphological phylogenetic
- analyses. *Mol. Biol. Evol.* **34**, 772–773 (2017).
- 563 42. F. Ronquist et al., MrBayes 3.2: efficient Bayesian phylogenetic inference and model choice across
- a large model space. Syst. Biol. **61**, 539–542 (2012).
- 565 43. C. Zhang, T. Stadler, S. Klopfstein, T. A. Heath, F. Ronquist, Total-evidence dating under the
- fossilized birth–death process. Syst. Biol. 65, 228–249 (2016).
- 44. R. Froese, D. Pauly, Eds. FishBase. World Wide Web electronic publication, version (10/2020).
- Available at www.fishbase.org
- 569 45. L. Cavin, P. L. Forey, Osteology and systematic affinities of *Palaeonotopterus greenwoodi* Forey
- 570 1997 (Teleostei: Osteoglossomorpha). Zool. J. Linn. Soc. 133, 25–52 (2001).
- 571 46. M. Friedman, The early evolution of ray-finned fishes. *Palaeontology* 58, 213–228 (2015).
- 572 47. J. T. Clarke, G. T. Lloyd, M. Friedman, Little evidence for enhanced phenotypic evolution in early
- teleosts relative to their living fossil sister group. *Proc. Natl. Acad. Sci. U.S.A.* 113, 11531–11536
- 574 (2016).
- 48. A. Rambaut, A. J. Drummond, D. Xie, G. Baele, M. A. Suchard, Posterior summarization in
- 576 Bayesian phylogenetics using Tracer 1.7. Syst. Biol. 67, 901–904 (2018).
- 577 49. S. Klopfstein, T. Spasojevic, Illustrating phylogenetic placement of fossils using RoguePlots: an
- 578 example from ichneumonid parasitoid wasps (Hymenoptera, Ichneumonidae) and an extensive
- 579 morphological matrix. *PLoS One* **14**, e0212942 (2019).
- 580 50. N. J. Matzke, Model selection in historical biogeography reveals that founder-event speciation is a
- 581 crucial process in island clades. *Syst. Biol.* **63**, 951–970 (2014).
- 51. R. H. Ree, S. A. Smith, Maximum likelihood inference of geographic range evolution by dispersal,
- local extinction, and cladogenesis. Syst. Biol. 57, 4–14 (2008).
- 52. F. Ronquist, Dispersal-vicariance analysis: a new approach to the quantification of historical

- 585 biogeography. Syst. Biol. 46, 195–203 (1997).
- 53. M. J. Landis, N. J. Matzke, B. R. Moore, J. P. Huelsenbeck, Bayesian analysis of biogeography
- when the number of areas is large. *Syst. Biol.* **62**, 789–804 (2013).
- 54. R. H. Ree, I. Sanmartín, Conceptual and statistical problems with the DEC+J model of founder-
- 589 event speciation and its comparison with DEC via model selection. J. Biogeogr. 45, 741–749 (2018).
- 590 55. K. V. Klaus, N. J. Matzke, Statistical comparison of trait-dependent biogeographical models
- indicates that Podocarpaceae dispersal is influenced by both seed cone traits and geographical
- 592 distance. Syst. Biol. 69, 61–75 (2020).
- 56. K. P. Burnham, D. R. Anderson, Model selection and multimodel inference—a practical
- *information-theoretic approach* (Springer, New York, NY, 2002).
- 595 57. J. Dupin et al., Bayesian estimation of the global biogeographical history of the Solanaceae. J.
- 596 Biogeogr. 44, 887–899 (2017).
- 597 58. J. D. Boyko, J. M. Beaulieu, Generalized hidden Markov models for phylogenetic comparative
- 598 datasets. *Methods Ecol. Evol.* **12**, 468–478 (2021).
- 599 59. L. J. Revell, phytools: an R package for phylogenetic comparative biology (and other things).
- 600 *Methods Ecol. Evol.* **3**, 217–223 (2012).
- 601 60. S. Lavoué, J. P. Sullivan, Simultaneous analysis of five molecular markers provides a well-
- supported phylogenetic hypothesis for the living bony-tongue fishes (Osteoglossomorpha:
- 603 Teleostei). *Mol. Phylogenet. Evol.* **33**, 171–185 (2004).
- 61. J. G. Inoue, Y. Kumazawa, M. Miya, M. Nishida, The historical biogeography of the freshwater
- knifefishes using mitogenomic approaches: a Mesozoic origin of the Asian notopterids
- 606 (Actinopterygii: Osteoglossomorpha). Mol. Phylogenet. Evol. 51, 486–499 (2009).
- 607 62. S. Lavoué *et al.*, Remarkable morphological stasis in an extant vertebrate despite tens of millions of
- 608 years of divergence. *Proc. Biol. Sci.* **278**, 1003–1008 (2011).
- 63. S. Lavoué et al., Comparable ages for the independent origins of electrogenesis in African and South
- American weakly electric fishes. *PLoS One* 7, e36287 (2012).
- 64. T. J. Near *et al.*, Resolution of ray-finned fish phylogeny and timing of diversification. *Proc. Natl.*

- 612 Acad. Sci. U.S.A. 109, 13698–13703 (2012).
- 65. B. Brown, C. Gaina, R. D. Müller, Circum-Antarctic palaeobathymetry: Illustrated examples from
- 614 Cenozoic to recent times. *Palaeogeogr. Palaeoclimatol. Palaeoecol.* 231, 158–168 (2006).
- 615 66. M. D. Ezcurra, F. L. Agnolín, A new global palaeobiogeographical model for the late Mesozoic and
- 616 early Tertiary. Syst. Biol. 61, 553–566 (2012).
- 617 67. H. Haddoumi et al., Guelb el Ahmar (Bathonian, Anoual Syncline, eastern Morocco): first
- continental flora and fauna including mammals from the Middle Jurassic of Africa. *Gondwana Res.*
- **29**, 290–319 (2016).
- 68. J. P. Tennant, P. D. Mannion, P. Upchurch, M. D. Sutton, G. D. Price, Biotic and environmental
- dynamics through the Late Jurassic–Early Cretaceous transition: evidence for protracted faunal and
- 622 ecological turnover. *Biol. Rev.* **92**, 776–814 (2017).
- 69. C. Heine, J. Zoethout, R. D. Müller, Kinematics of the South Atlantic rift. Solid Earth 4, 215–253
- 624 (2013).
- 70. L. Taverne, Les ostéoglossomorphes marins de l'Éocène du Monte Bolca (Italie): *Monopteros* Volta
- 626 1796, Thrissopterus Heckel, 1856 et Forevichthys Taverne, 1979. Considérations sur la phylogénie
- 627 des téléostéens ostéoglossomorphes. Studi e Ricerche sui Giacimenti Terziari di Bolca, VII –
- 628 *Miscellanea Paleontologica* **4**, 67–158 (1998).
- 71. S. Lavoué, Testing a time hypothesis in the biogeography of the arowana genus Scleropages
- 630 (Osteoglossidae). J. Biogeogr. 42, 2427–2439 (2015).
- 631 72. R. Betancur-R, G. Ortí, R. A. Pyron, Fossil-based comparative analyses reveal ancient marine
- ancestry erased by extinction in ray-finned fishes. *Ecol. Lett.* **18**, 441–450 (2015).
- 73. D. D. Bloom, N. R. Lovejoy, On the origins of marine-derived freshwater fishes in South America.
- 634 *J. Biogeogr.* 44, 1927–1938 (2017).
- 74. A. Ghezelayagh et al., Prolonged morphological expansion of spiny-rayed fishes following the end-
- 636 Cretaceous. *Nat. Ecol. Evol.* **6**, 1211–1220 (2022).
- 75. J. Zachos, M. Pagani, L. Sloan, E. Thomas, K. Billups, Trends, rhythms, and aberrations in global
- 638 climate 65 Ma to present. *Science* **292**, 686–693 (2001).

- 639 76. M. Friedman, L. C. Sallan, Five hundred million years of extinction and recovery: a Phanerozoic
- survey of large-scale diversity patterns in fishes. *Palaeontology* **55**, 707–742 (2012).
- 77. A. Capobianco et al., Large-bodied sabre-toothed anchovies reveal unanticipated ecological
- diversity in early Palaeogene teleosts. R. Soc. Open Sci. 7, 192260 (2020).
- 78. A. M. Murray, The Palaeozoic, Mesozoic and early Cenozoic fishes of Africa. Fish Fish. (Oxf.) 1,
- 644 111–145 (2000).
- 79. R. B. Benson, R. Butler, R. Close, E. Saupe, D. L. Rabosky, Biodiversity across space and time in
- the fossil record. *Curr. Biol.* **31**, R1225–R1236 (2021).
- 80. C. O'Donovan, A. Meade, C. Venditti, Dinosaurs reveal the geographical signature of an
- 648 evolutionary radiation. *Nat. Ecol. Evol.* **2**, 452–458 (2018).
- 81. J. D. Gardner, K. Surya, C. L. Organ, Early tetrapodomorph biogeography: controlling for fossil
- record bias in macroevolutionary analyses. C. R. Palevol. 18, 699–709 (2019).
- 651 82. D. Silvestro et al., Fossil biogeography: a new model to infer dispersal, extinction and sampling
- from palaeontological data. *Philos. Trans. R. Soc. B* **371**, 20150225 (2016).
- 653 83. T. Hauffe, M. M. Pires, T. B. Quental, T. Wilke, D. Silvestro, A quantitative framework to infer the
- 654 effect of traits, diversity and environment on dispersal and extinction rates from fossils. *Methods*
- 655 *Ecol. Evol.* **13**, 1201–1213 (2022).
- 84. M. Landis, E. J. Edwards, M. J. Donoghue, Modeling phylogenetic biome shifts on a planet with a
- 657 past. Syst. Biol. **70**, 86–107 (2021).
- 658 85. J. Andréoletti et al., The Occurrence Birth-Death Process for combined-evidence analysis in
- macroevolution and epidemiology. Syst. Biol. 71, 1440–1452 (2022).
- 660 86. S. Varela, K. S. Rothkugel. Mapast: combine paleogeography and paleobiodiversity. R package
- version 0.1 (2018). Available at https://github.com/macroecology/mapast
- 87. T. M. Berra, Freshwater Fish Distribution (The University of Chicago Press, Chicago, IL, 2007).



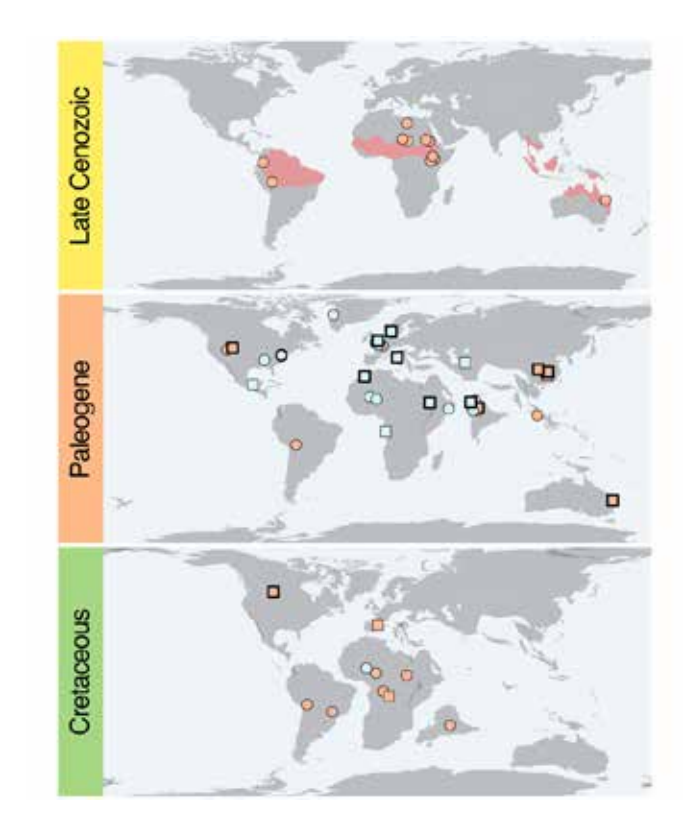


Figure 1. Geographic distribution of extinct and extant osteoglossid bonytongues. Fossil occurrences are divided by preservation state (*circles*: fragmentary and disarticulated fossils; *squares*: articulated fossils) and paleoenvironment (*orange fill*: freshwater deposits; *light blue fill*: marine deposits). Fossil occurrences with thicker borders indicate where the extinct osteoglossids included in the phylogenetic and biogeographic analyses have been found. The red area in the late Cenozoic map displays the current geographic distribution of extant osteoglossids. Paleogeographic maps at 0, 50 and 85 Ma were generated in the R package mapast under the MULLER2016 model [86]. Fossil osteoglossid occurrences from [26,30,31]. Geographic distribution of extant osteoglossids from [87].

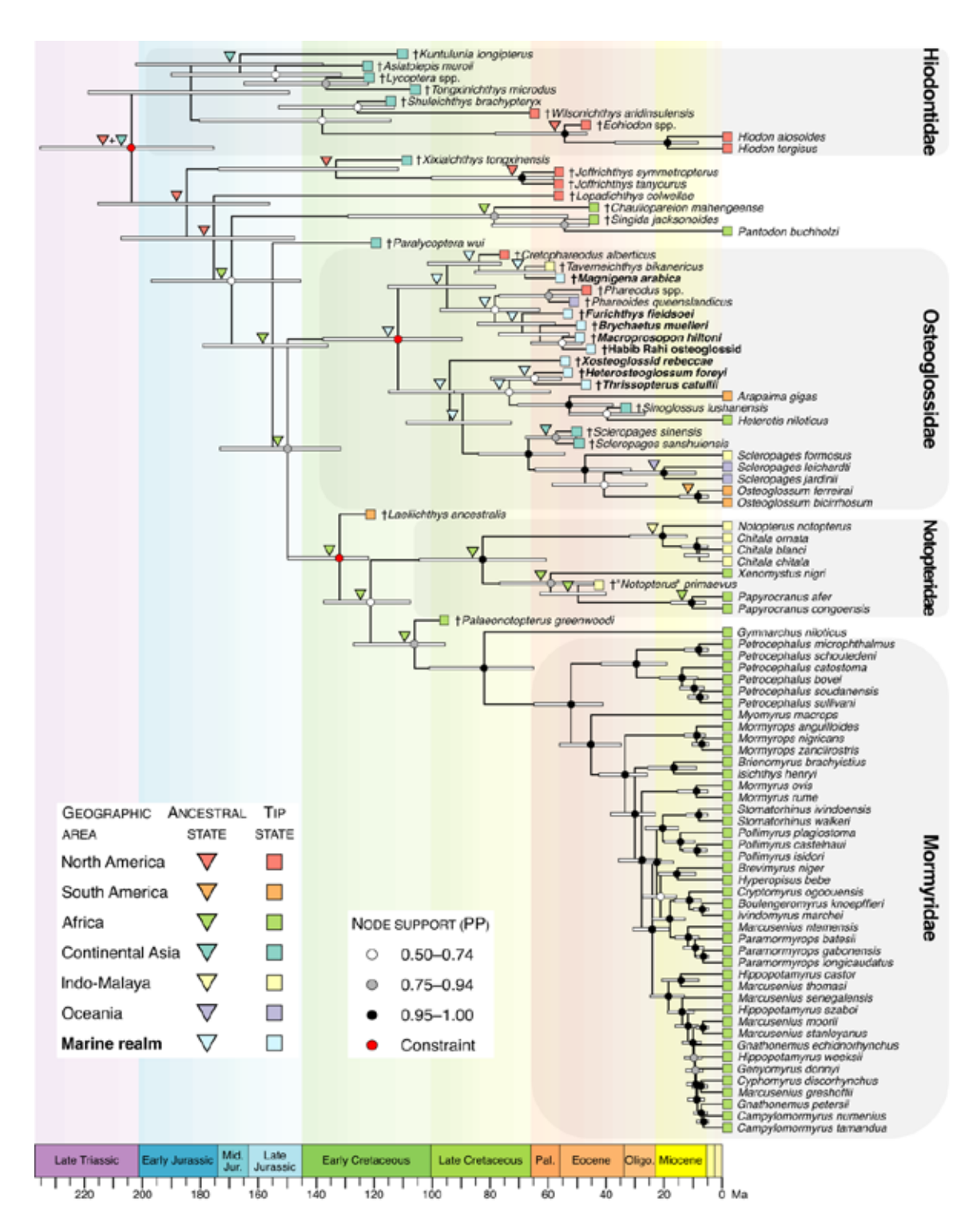


Figure 2. Time-calibrated phylogeny of Osteoglossomorpha. The phylogeny plotted here is the 'AllCompat' summary consensus tree from the Bayesian total-evidence analysis. Tips are colored according to geographic distribution. Taxa found in marine settings are highlighted in boldface. Colored triangles at internal nodes

represent the most likely ancestral geographic area under the DEC+*j* model when it is at least 3.2 times more likely than the second-most likely geographic area, indicating substantial strength of evidence under a Bayes factor framework. Colored triangles at internal nodes for which all descendant tips and the immediately ancestral node inhabit the same area were masked to avoid figure cluttering. Circles at internal nodes indicate node support as Bayesian posterior probabilities of clades when equal to or larger than 0.50. White bars represent 95% highest posterior densities (HPD) of node ages. Highlighted clades refer to the total-group (crown group + stem group). Ma = million years ago.

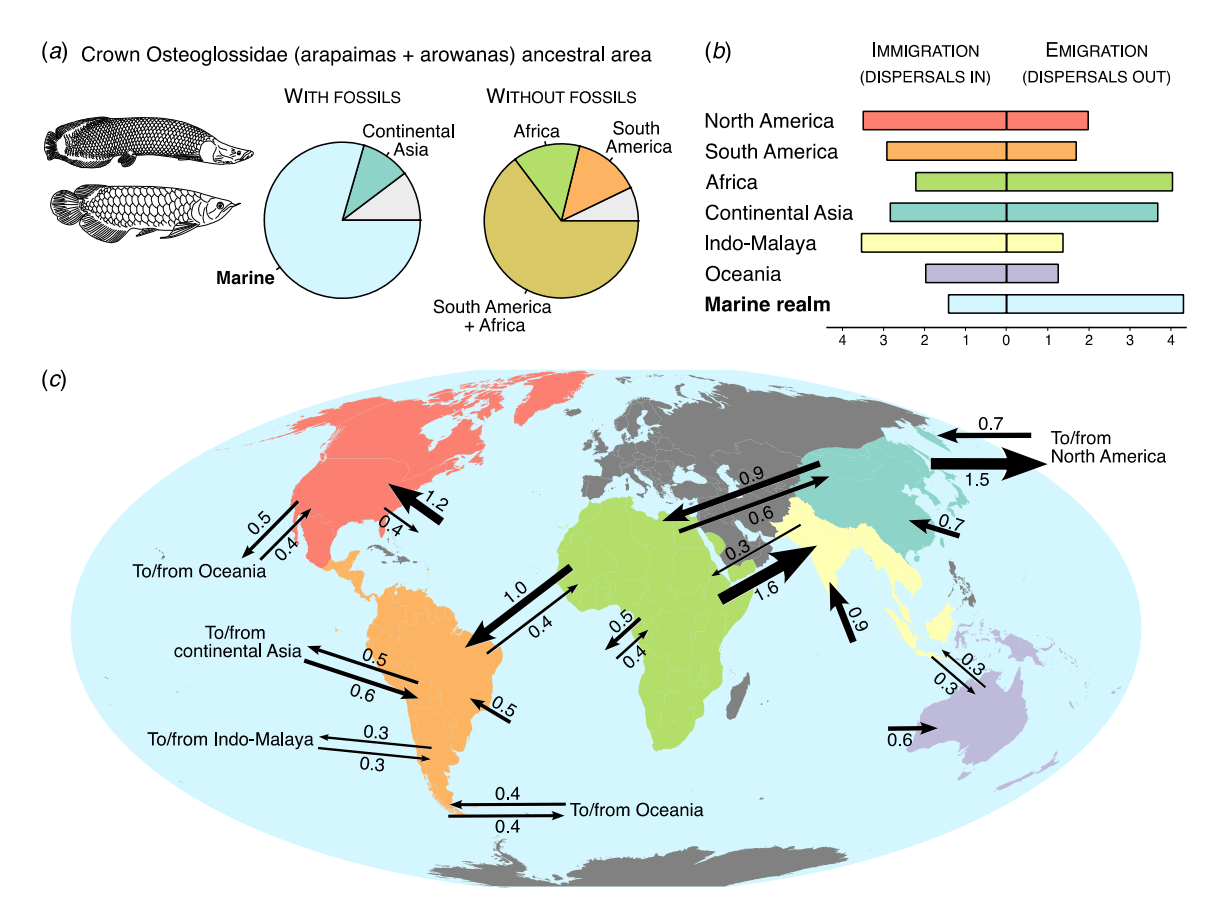


Figure 3. Historical biogeography of bonytongue fishes integrated over phylogenetic uncertainty. Marginal probabilities and numbers of dispersal events shown in this figure have been integrated over a random sample of 200 phylogenies from the Bayesian posterior distribution. (a) Marginal probabilities of ancestral biogeographic area under the DEC+j model for crown Osteoglossidae when fossils are included in (left) or excluded from the analysis (right). (b) Average number of dispersal events into (immigration) and from (emigration) biogeographic areas, calculated under biogeographical stochastic mapping (BSM) and integrated over phylogenetic uncertainty. (c) Directionality of dispersal between biogeographic areas, calculated under BSM. Arrow thickness is proportional to the average number of dispersal events, indicated by the number next to the arrow. Arrows from one area to another are not shown when the average number of dispersal events is lower than 0.3.

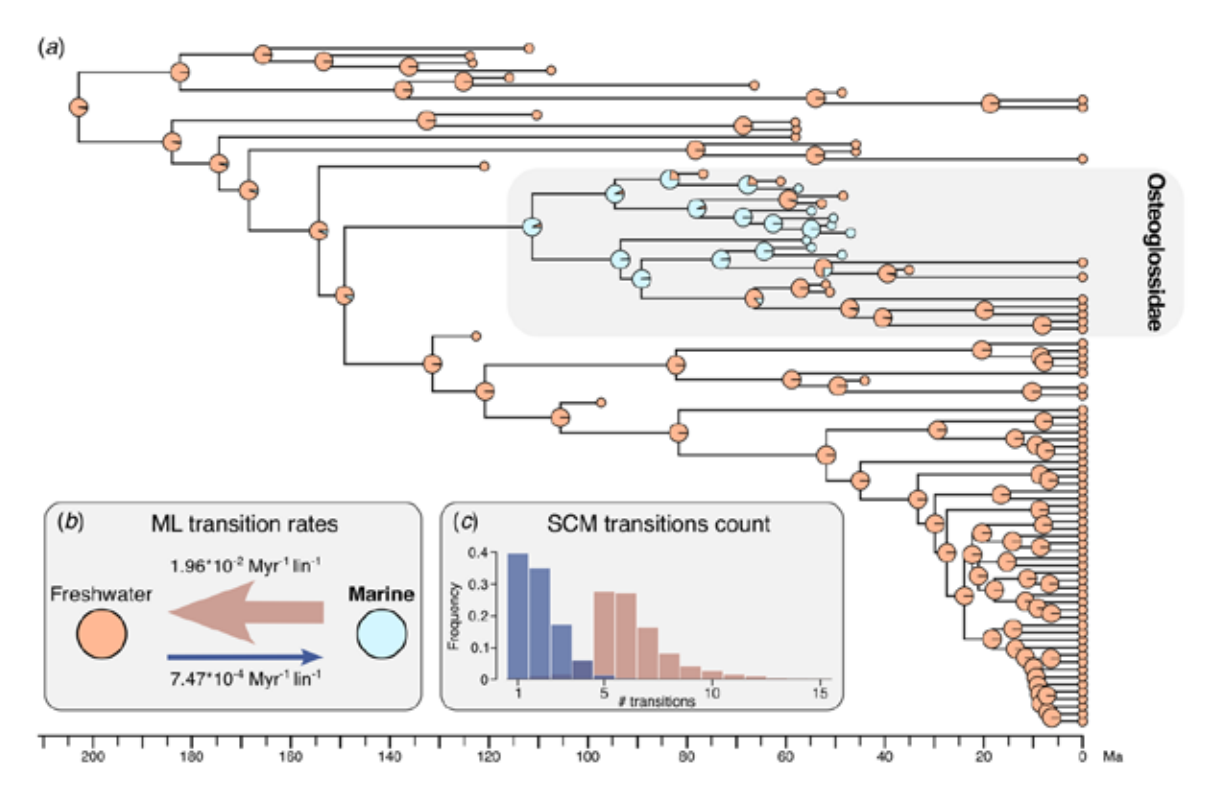


Figure 4. Ancestral habitat estimation for bonytongue fishes. (*a*) Marginal ancestral states under an all-rates-different (ARD) model on the Bayesian consensus tree of Osteoglossomorpha. Orange fill indicates freshwater environment, while light blue fill indicates marine environment. Tip identities are the same as in figure 2, with total-group Osteoglossidae highlighted in light gray. (*b*) Maximum likelihood estimates of transition rates between freshwater and marine environments, expressed per million years per lineage (Myr lin-1). (*c*) Distribution of the inferred number of environmental transitions under stochastic character mapping (SCM) on the Bayesian consensus tree of Osteoglossomorpha. Freshwater-to-marine transitions are in dark blue, marine-to-freshwater transitions are in brown.

- Fossils indicate marine dispersal in osteoglossid fishes, a classic example of continental vicariance
- **Supplemental Material**

4 Supplemental text

5

6

Material and methods

- 7 Institutional abbreviations. FMNH, The Field Museum, Chicago, IL, USA; FUM, Fur Museum, Fur,
- 8 Denmark; IGUP, Istituto Geologico dell'Università di Padova, Padova, Italy; MCSNV, Museo Civico di
- 9 Storia Naturale, Verona, Italy; NHMUK, The Natural History Museum, London, UK; UMMP, University of
- 10 Michigan Museum of Paleontology, Ann Arbor, MI, USA; UMMZ, University of Michigan Museum of
- Zoology, Ann Arbor, MI, USA; UQ, University of Queensland, Brisbane, Australia.

- 13 Morphological dataset. A modified version of the morphological character matrix from [1] was used as the
- morphological partition for a total-evidence (morphology + DNA) phylogenetic analysis. We added the
- following taxa to the Capobianco *et al.* (in press) morphological matrix:
- 16 Notopterus notopterus (Notopteridae; extant, Indomalayan realm), with characters scored on the basis of
- 17 [2] and [3];
- 18 Gymnarchus niloticus (Gymnarchidae; extant, Afrotropical realm), with characters scored on the basis of
- 19 [4] and μ CT scan of UMMZ 195003;
- 20 †Heterosteoglossum foreyi (Osteoglossidae; Ypresian, Denmark), based on personal observations of FUM-
- 21 N 28904 and NHMUK PV P23946, and on [5];
- 22 †Notopterus primaevus (Notopteridae; Eocene, Sumatra), based on personal observations and μCT scan of
- 23 NMHUK PV P47512;
- 24 †Phareodus (=Phareoides) queenslandicus (Osteoglossidae; Thanetian-Ypresian, Australia), based on
- personal observations of FMNH PF 14254 (holotype cast) and UQ F.14960 (cast at AMNH), and on [6–8];
- 26 † Taverneichthys bikanericus (Osteoglossidae; Paleocene, India), based on [9,10];
- 27 †Thrissopterus catullii (Osteoglossidae; Ypresian, Italy), based on personal observations of IGUP 8839-
- 28 8840 and MCSNV IG 91137-91138, and on [11];

- 29 †Xosteoglossid rebeccae (?Osteoglossidae; Ypresian, Denmark), based on personal observations of FUM-
- 30 N 28905 and on [5];
- 31 †Scleropages sinensis (Osteoglossidae; Ypresian, China), based on [12];
- 32 †Scleropages sanshuiensis (Osteoglossidae; Ypresian, China), based on [13];
- 33 † Cretophareodus alberticus (?Osteoglossidae; Campanian, Canada), based on [14];
- 34 †Kuntulunia longipterus (Osteoglossomorpha incertae sedis; Aptian–Albian, China), based on [15];
- 35 † Asiatolepis muroii (stem Osteoglossomorpha; Barremian–early Aptian, China), based on [16];
- 36 †Tongxinichthys microdus (stem Osteoglossomorpha; Albian, China), based on [17];
- 37 †Magnigena arabica (Osteoglossidae; Thanetian, Saudi Arabia), based on personal observations and μCT
- 38 scan of NHMUK PV OE PAL 2007-1, and on [18];
- 39 UMMP GSP-UM field no. 1981292, labeled as 'Habib Rahi osteoglossid' (undescribed Osteoglossidae;
- 40 Habib Rahi Formation, Lutetian, Pakistan), based on personal observations and μCT scan.
- 41 Several of these taxa are particularly relevant for their age, paleogeographic and paleoenvironmental setting,
- and potential taxonomic affinities, yet they have never been included in a phylogenetic analysis before.
- 44 *Micro-computed tomography.* In addition to the comparative material listed in Capobianco *et al.* (in press),
- 45 the following specimens of extinct and extant osteoglossomorphs were imaged using a Nikon XT H 225ST
- 46 industrial μCT scanner at the University of Michigan CTEES facility (Computed Tomography in Earth &
- 47 Environmental Sciences):

- 48 †Magnigena arabica, NHMUK PV OE PAL 2007-1. Voltage, 190 kV; current, 190 μA; filter, copper 2.5
- 49 mm; reflection target, tungsten; effective pixel size, 30.17 μm.
- [†]Notopterus primaevus, NMHUK PV P47512. Voltage, 185 kV; current, 200 μA; filter, copper 3.5 mm;
- 51 reflection target, tungsten; effective pixel size, 50.05 μm.
- 52 'Habib Rahi osteoglossid', UMMP GSP-UM field no. 1981292. Voltage, 185 kV; current, 180 μA; filter,
- 53 copper 2.8 mm; reflection target, tungsten; effective pixel size, 119.33 μm.

Gymnarchus niloticus, UMMZ 195003. Voltage, 70 kV; current, 220 μA; filter, none; reflection target, tungsten; effective pixel size, 40.05 μm.

56

57

58

59

60

61

62

63

64

65

66

67

68

69

70

71

72

73

74

75

76

77

78

79

54

55

Molecular dataset. The molecular data matrix was assembled by integrating part of the genomic dataset of [19] with semi-automated extraction of DNA sequences from Genbank (via the NCBI platform) and BOLD (Barcode Of Life Data system), using functions from the R package reqPhylo [20]. A list of extant osteoglossomorph species was compiled from FishBase [21] and checked through the NCBI taxonomic database to extract their NCBI taxonomic ID. Extant outgroups (Amia calva, Elops saurus, and Dorosoma cepedianum) were added to this list. DNA sequences belonging to the listed species were extracted from Genbank and BOLD; after removing microsatellites and unassigned DNA, a species-by-gene matrix was assembled to identify which genetic markers maximize taxonomic coverage. Following the criterion of maximum taxonomic coverage, four DNA markers were selected, two of which are protein-coding mitochondrial markers, (coI, cytb) and the other two non-protein-coding mitochondrial regions (12S rRNA, 16S rRNA). After removal of potential outlier sequences, one sequence per species and marker was selected using the SelBestSeq function. Multiple alignments of these sequences were performed both with MAFFT [22] and MUSCLE [23]. Alignment quality was assessed in MUMSA [24] by calculating the multiple overlap score of each alignment (MOS); alignments with the highest MOS for each marker were picked for the following steps. Poorly aligned positions were trimmed with GBLOCKS [25]. Trimmed alignments were visually inspected with AliView [26] and manually edited when needed. In addition to the four mitochondrial markers, we extracted eight protein-coding nuclear markers (rag1, rag2, glyt, ficd, megf8, pdzd8, suox, vcpip1) from the genome-wide exon alignments of [19]. For the three outgroups (A. calva, E. saurus, and D. cepedianum), nuclear markers were downloaded from Genbank when available. Additionally, ragl sequences for Notopterus notopterus and Pantodon buchholzi and the rag2 sequence for Papyrocranus afer were also downloaded from Genbank, as they were missing from the alignments of [19]. The final molecular dataset comprised 14,084 nucleotides for 63 OTUs—including all extant osteoglossomorph genera and 23.4% of all extant osteoglossomorph species—with 87% matrix completeness at the marker level.

- 82 Comments on character scoring for some taxa.
- 83 †Brychaetus muelleri was scored based on the μCT scans of NHMUK PV P641 and NHMUK PV P26758,
- and on personal observation of the other comparative material listed in [1].
- 85 Character (8): Parasphenoid teeth. Despite the presence of teeth on the parasphenoid in most osteoglossids
- 86 (including †*Phareodus*), no parasphenoid teeth can be seen in the µCT scans of NHMUK PV P641 and
- NHMUK PV P26758. Thus, we scored this character as absent ('0').
- 88 Character (14): Basioccipital process of the parasphenoid. A divided or paired basioccipital process of the
- 89 parasphenoid is clearly visible in the μCT scan of NHMUK PV P26758. Thus this character is scored as
- 90 divided ('0').
- 91 Character (15): Ventral occipital groove. This character was scored as present ('0'), as μCT scans of NHMUK
- 92 PV P641 and NHMUK PV P26758 show a ventral occipital groove of similar position (immediately posterior
- to the basipterygoid process) and size to the one observed in †*Phareodus* [27].
- 94 Character (16): Intercalar. An intercalar is clearly visible in the µCT scan of NHMUK PV P641, thus this
- character was scored as present ('0').
- 96 Character (17): Foramen/foramina for anteroventral lateral line nerve plus cranial nerve V. The μCT scan of
- NHMUK PV P641 shows that the prootic completely surrounds the foramen for the anteroventral lateral line
- 98 nerve plus cranial nerve V, antero-dorsally to the anterior entrance for the jugular canal. This is a primitive
- condition for teleosts, and it is also seen in all extant osteoglossids except for Arapaina [3]. Consequently,
- we scored this character as 'in the prootic' ('0').
- 101 Character (18): Suture between the parasphenoid and sphenotic. The µCT scan of NHMUK PV P641 does
- not show contact between the parasphenoid and the sphenotic. Thus, this character was scored as 'absent'
- 103 ('0').
- 104 Character (19): Foramen for cranial nerve VI. As observed in the μCT scan of NHMUK PV P641, the
- foramen for cranial nerve VI opens within the prootic bridge, hence this character was scored as '0'.
- 106 Character (22): Number of bones in the infraorbital series, not including the dermosphenotic or the antorbital
- if present. Contrary to [28] which illustrated three infraorbital bones, we observed four infraorbital bones in
- † † *Brychaetus*, as in most bonytongue fishes. Thus, this character was scored as 'four' ('1').

109 Character (27): Posterior extent of the fossa on the neurocranium for the hyomandibula. We observed in the 110 μCT scan of NHMUK PV P641 that the intercalar is included in the posterior portion of the fossa for the 111 hyomandibula, albeit it contributes only marginally to the fossa. Consequently, this character was scored as 112 'formed of pterotic and intercalar' ('1'). 113 Character (28): Neurocranial heads of the hyomandibula. Two separate neurocranial heads of the 114 hyomandibula can be seen in NHMUK PV P26758, illustrated in Fig. 13 of [1]. Thus, this character was 115 scored as 'two heads, separate' ('1'). 116 Character (37): Ascending process of the premaxilla. The premaxilla seen in NHMUK PV 43021 bears an 117 ascending process that is only slightly developed, more similar to the condition seen in Osteoglossum and 118 Scleropages than the one seen in †Phareodus. Thus, this character was scored as only slightly developed if 119 at all ('1'). 120 Character (45): Bony elements associated with the second ventral gill arch. Ventromedial bony processes on 121 the second hypobranchial can be seen in the µCT scan of NHMUK PV P641. Thus, we scored this character 122 as 'present as a bony process on the second hypobranchial' ('2'). 123 Character (46): Toothplates associated with basibranchial 4. No posterior basibranchial toothplate can be 124 seen in the µCT scan of NHMUK PV P641, so this character was scored as 'absent' ('1'). 125 126 †Furichthys fieldsoei was scored based on personal observation of the holotype (FUM-N 1440) and referred 127 specimen (FUM-N 1848A), and on the description in [5]. 128 Character (2): Extrascapular. [5] reports a broad and flat extrascapular in the referred specimen FUM-N 129 1848A. However, after personal observation of the specimen, the identity of the element identified by [5] as 130 an extrascapular is unclear. The surface texture of this element is somewhat similar to that of the body scales 131 preserved in the same specimen, raising the possibility that it could instead be a large nuchal scale similar to 132 the ones seen in extant osteoglossids such as *Heterotis* and *Scleropages*. Ultimately, this character was scored 133 as uncertain ('?'). 134 Character (8): Parasphenoid teeth. [5] reports a potential parasphenoid tooth patch postero-dorsally to the 135 vomer in the holotype. After personal observation of the holotype, we cannot determine whether the small

136 tooth patch described by [5] belongs to the parasphenoid, to the vomer, or to an element of the palate. Hence, 137 this character was scored as uncertain ('?'). 138 Character (16): Intercalar. This character was scored as '0' (present), as the intercalar can be identified as a 139 small triangular element of the posterior part of the braincase on the right side of the holotype. This bone is 140 not mentioned in the description by [5]. 141 Character (27): Posterior extent of the fossa on the neurocranium for the hyomandibula. While the 142 neurocranial heads of the hyomandibula is clearly visible in the referred specimen FUM-N 1848A, the portion 143 of the braincase that articulates with them is not well preserved, and the identity of the bones that make up 144 the fossa for the hyomandibula is not clear. Thus, this character was scored as uncertain ('?'). 145 Characters (47) and (48): Basihyal toothplate. [5] identifies a basihyal toothplate in the ventral portion of the 146 left side of the holotype. Given the symmetrical shape of this tooth-bearing element with a ventral concavity, 147 we interpret it as a basibranchial toothplate exposed in transversal cross section. Thus, we could not determine 148 the presence and shape of the basihyal toothplate, and these characters were scored as uncertain ('?'). 149 Character (76): Opercle shape dorsal to facet for articulation with hyomandibula. The opercle is well 150 preserved in the referred specimen FUM-N 1848A. [5] drew the outline of the opercle as dorsally truncated 151 just above the level of its articular facet. However, the opercle appears to extend dorsally further than what 152 is drawn in [5], narrowing into a rounded shape. Thus, this character was scored as '0' (rounded). 153 Character (93): Postero-dorsal flange of the angular. This feature is apparently absent when observing the 154 holotype. However, the holotype of the closely related species †Macroprosopon hiltoni [1] preserves the 155 postero-dorsal flange of the angular on the right side, but not on the left side, of the specimen, despite 156 preserving the angular on both sides. This suggests that this flange might break off from the angular rather 157 easily during taphonomic processes. Thus, we decided to score this character as uncertain ('?'). 158 159 †Heterosteoglossum forevi was scored based on personal observation of the holotype FUM-N 28904 and 160 referred specimen NHMUK PV P23946, and on the description in [5]. 161 Character (1): Temporal fossa. This character was scored as uncertain ('?') because it is unclear which bones 162 border the temporal fossa.

- 163 Character (5): Length of frontal bone. While the suture between frontal and parietal is not easily identifiable, 164 it appears that the great majority of the skull roof is made up by nasals and frontals, with parietals restricted 165 to the posteriormost portion of the skull roof. Thus, this character was scored as '0' (over twice as long as 166 parietal).
- 167 Character (25): Palatoquadrate area behind and below orbit. The infraorbitals do not seem to be preserved,
 168 thus it is not possible to determine whether the infraorbitals completely covered the palatoquadrate area
 169 behind the orbit or not. Consequently, this character was scored as uncertain ('?'). However, because the
 170 region between orbit and preopercle is very short, it is more likely than not that the palatoquadrate area would
 171 have been fully covered by the infraorbitals.
- 172 Character (41): Mandibular canal. The character state '0' (enclosed in a bony tube) can be inferred by the
 173 presence of lateral pores for the canal in the lower jaw and absence of a mandibular groove.
- 174 Character (65): Number of principal caudal fin rays. [5] reports 18 principal caudal fin rays (9 + 9) in the 175 referred specimen NHMUK P23946, a specimen preserving the caudal skeleton and a small portion of the 176 caudal fin. However, after personal observation of the specimen, it is more likely that 17 principal caudal fin 177 rays (8 + 9) make up the caudal fin. Thus, this character was scored as '2' (17 or fewer).
- 178 Character (66): Uroneurals. This character was scored as uncertain ("?") because a small element dorsal to
 179 the second ural centrum could represent either a uroneural or an epural.
- 181 Gymnarchus niloticus was scored based on the μCT scan of UMMZ 195003 and on [4].

188

182 Character (22): Number of bones in the infraorbital series, not including the dermosphenotic or the antorbital
183 if present. In previous iterations of the character matrix used for this study (e.g. [1]), this character had two
184 states: five ('0') or four ('1') infraorbitals. *Gymnarchus* is unique among osteoglossomorph in possessing a
185 very large number of tubular infraorbital elements—between 8 and 11 for [29] and between 12 and 13 for
186 [4], excluding the antorbital. Consequently, to score *Gymnarchus* for this character, we added a third state:
187 six or more ('2').

Scleropages leichardti and Scleropages jardinii were scored based on [3,30,31].

Character (31): Autopalatine bone. While an autopalatine bone is absent in *S. formosus* (and in most other osteoglossomorphs), it is present in *S. leichardti* [3, 30]. The state of this character is unknown in *S. jardinii*.

Thus, this character was scored as present ('0') in S. leichardti and uncertain ('?') in S. jardinii.

Character (71): Number of hypurals. Both *S. leichardti* and *S. jardinii* have seven hypurals (state '0'), one more than in *S. formosus* (state '1': six or fewer) [31].

195

196

197

190

191

193

194

More thorough morphological redescriptions of †*Magnigena arabica* and †*Notopterus primaevus*, as well as a first description of the Habib Rahi osteoglossid, are currently being undertaken by the authors of this study.

198

199

Results

200

201

202

203

204

205

206

207

208

209

210

211

212

213

214

215

216

Phylogenetic position of extinct non-osteoglossid bonytongue taxa. An ensemble of Early Cretaceous Chinese taxa grouped together in the family †Lycopteridae (†Asiatolepis, †Lycoptera, and †Tongxinichthys) are more likely to be early-diverging Hiodontiformes (total-group Hiodontidae), but both a stem Osteoglossomorpha or a stem Osteoglossiformes position cannot be excluded (posterior probability > 0.1). Another Early Cretaceous Chinese taxon, †Kuntulunia, occupies a similar phylogenetic position. The Early Cretaceous †Shuleichthys and the Late Cretaceous †Wilsonichthys are almost always recovered as stem Hiodontidae. The early Eocene †Eohiodon and extant Hiodon species form a strongly supported North American clade. In fact, †Eohiodon has been synonymized with Hiodon by some authors [32]. †Xixiaichthys and the two species of † Joffrichthys are most likely stem Osteoglossiformes or members of Hiodontiformes. The deep-bodied †Lopadichthys from the Paleocene of North America is one of the most poorly resolved taxon in our phylogeny, with possible placements including stem Osteoglossiformes, crown Osteoglossiformes as an early-diverging relative of *Pantodon*, and Hiodontiformes. Contrary to previous phylogenetic analyses [33,34; but see 1], the Early Cretaceous †*Paralycoptera* from China is recovered as an osteoglossiform, with possible positions including the osteoglossiform stem, the lineage leading to Pantodon, sister to Osteoglossidae + Notopteroidea, and stem Osteoglossidae. The early Eocene †Chauliopareion and †Singida from Tanzania are always placed on the lineage leading to Pantodon (stem Pantodontidae). The Early Cretaceous Brazilian †Laeliichthys is either sister to the Notopteridae + Mormyridae + Gymnarchus clade, or a stem notopterid. The Eocene †Notopterus primaevus from Sumatra is always reconstructed as a notopterid, and most often as being more closely aligned to extant African knifefishes (Papyrocranus and Xenomystus) than to extant Asian knifefishes (Notopterus and Chitala). The mid-Cretaceous †Palaeonotopterus from Morocco represents most likely a stem member of the Mormyridae + Gymnarchus clade, or alternatively of the Notopteridae + Mormyridae + Gymnarchus clade. A stem notopterid position, originally proposed for this taxon [35,36], is recovered in fewer than 7% of posterior trees.

Comments on notopterid biogeography. We found the ancestral geographic area for crown notopterid knifefishes to be uncertain between Africa and Indo-Malaya (76.3% probability Africa, 23.1% probability Indo-Malaya). Previous hypotheses about the present-day disjunct distribution of notopterids include an Africa–India vicariance scenario [37], a sweepstakes dispersal from Africa to India across the Mozambique Channel [38,39], and an overland dispersal from India to Africa after the collision between Africa and Eurasia in the late Cenozoic [40]. Our divergence time estimates and biogeographic analysis reject the vicariance scenario and favor the Africa-to-India dispersal hypothesis. However, the inferred position of the Sumatran †Notopterus primaevus as more closely related to extant African notopterids than to Asian species is unexpected and might suggest either two distinct dispersals from Africa, or a single dispersal from Southeast Asia to Africa if †N. primaevus is sister to all African taxa (Xenomystus + Papyrocranus). Under the latter hypothesis, the overland dispersal scenario with a relatively recent origin of African notopterids cannot be rejected. A comparative morphological reassessment of †N. primaevus is necessary to better elucidate the biogeographic history of notopterid knifefishes.

Biogeographic analysis without 'marine' as a biogeographic area. To test how alternative biogeographic area definitions impact our results, an additional biogeographic analysis was set up with a different scoring scheme for marine taxa. Instead of considering the marine realm as an additional geographic area, extinct taxa found in marine deposits were scored as belonging to the continental biogeographic regions where their fossils have been found in. All other settings were kept the same.

As in the 'marine-as-area' analysis, the DEC + j model was strongly favored compared to the other five models tested in BioGeoBEARS. Ancestral area reconstructions obtained with the two scoring schemes are compatible with each other (Fig. S6). However, some nodes within Osteoglossiformes that were reconstructed as ancestrally African with strong support under the 'marine-as-area' coding scheme are instead uncertain when 'marine' is not considered as a biogeographic area. Moreover, the nodes within Osteoglossidae that were reconstructed as ancestrally marine under the 'marine-as-area' coding scheme are either uncertain, or with substantial support towards a North American or European ancestral area (Fig. S6).

Data availability statement. Morphological and molecular character matrices, MrBayes scripts, MCMCMC log and tree files, tree files of the consensus tree and of the 200 sampled trees from the posterior, BioGeoBEARS and other R packages scripts, and BioGeoBEARS output files are available in a private Dryad repository that will be made public upon publication. Temporary URL for dataset download for peer review: https://datadryad.org/stash/share/81Hv4f1GPrJUYBRsgjgdV11xJtJ3pEQk7yFD7QBb7M8.

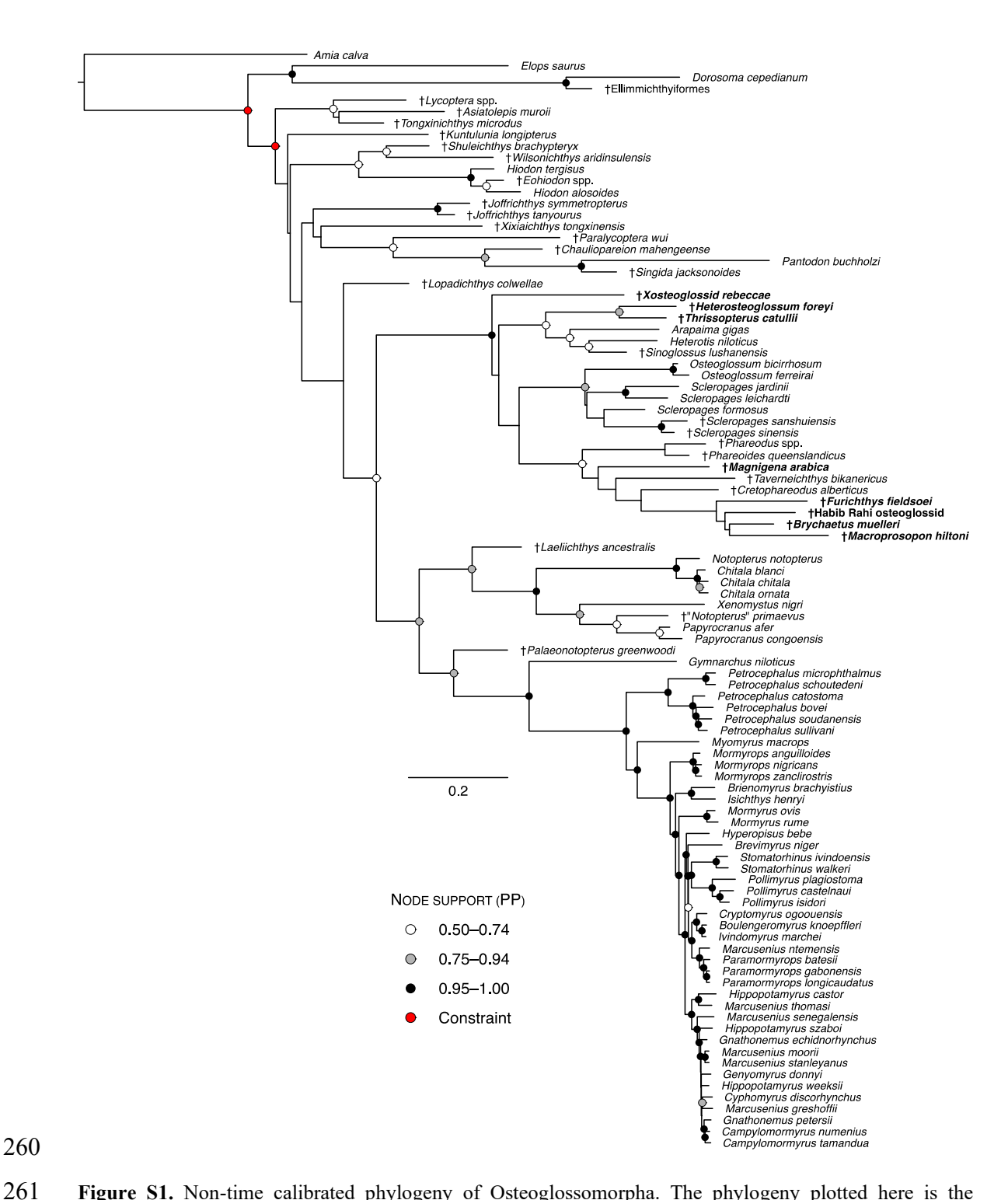


Figure S1. Non-time calibrated phylogeny of Osteoglossomorpha. The phylogeny plotted here is the 'AllCompat' summary consensus tree from the Bayesian unrooted, non-time calibrated analysis. Outgroup taxa are included, and the tree is rooted *a posteriori* at *Amia calva*. Taxa found in marine settings are highlighted in boldface. Circles at internal nodes indicate node support as Bayesian posterior probabilities of clades when equal to or larger than 0.50. Scale bar unit is average number of substitutions per site.

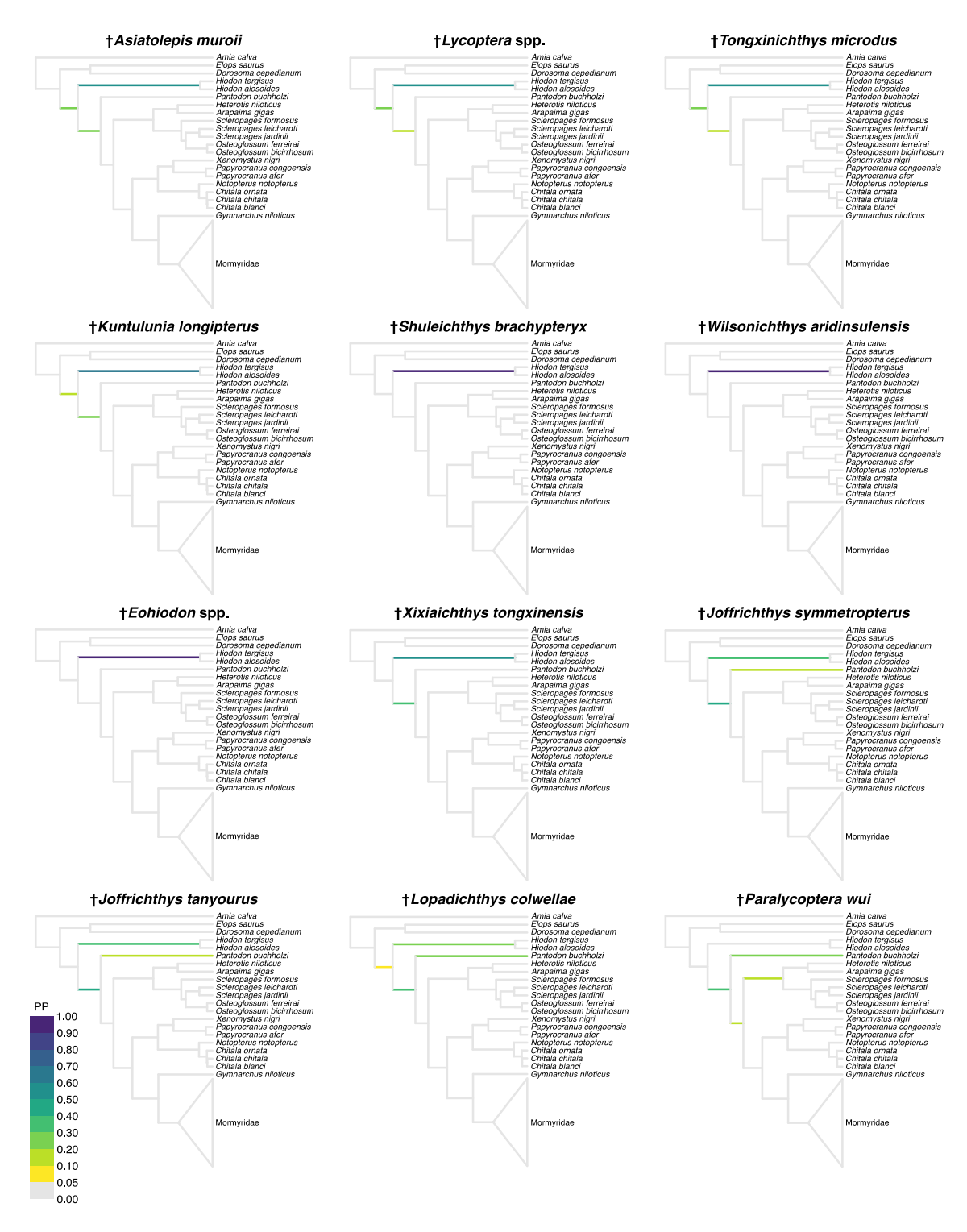


Figure S2 (*part one*). Phylogenetic position of extinct taxa in respect to extant ones across the Bayesian posterior distribution of time-calibrated trees. Mormyrid species were collapsed for clarity, as no fossil was ever reconstructed to fall within crown Mormyridae. PP = posterior probability.

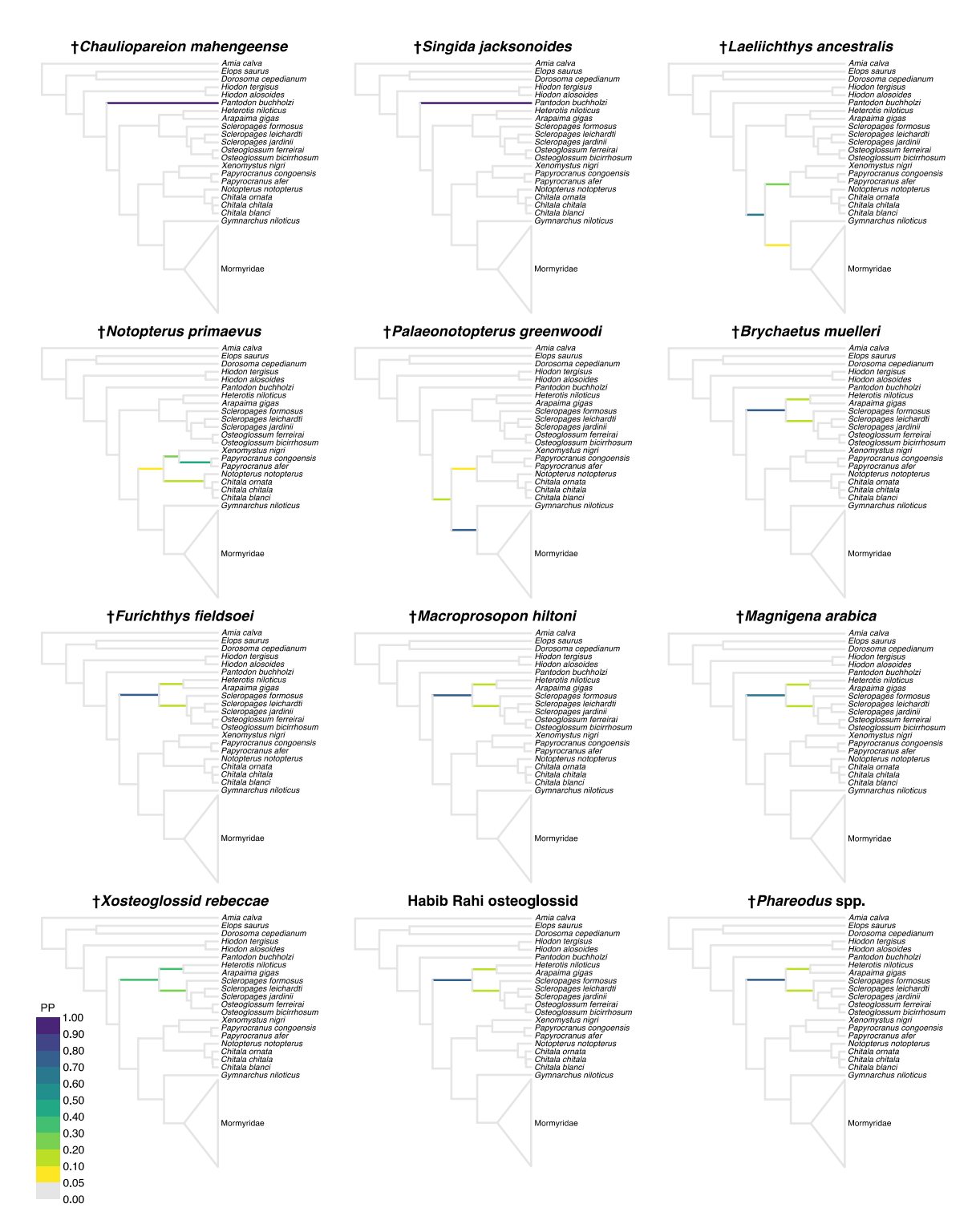


Figure S2 (*part two*). Phylogenetic position of extinct taxa in respect to extant ones across the Bayesian posterior distribution of time-calibrated trees. Mormyrid species were collapsed for clarity, as no fossil was ever reconstructed to fall within crown Mormyridae. PP = posterior probability.

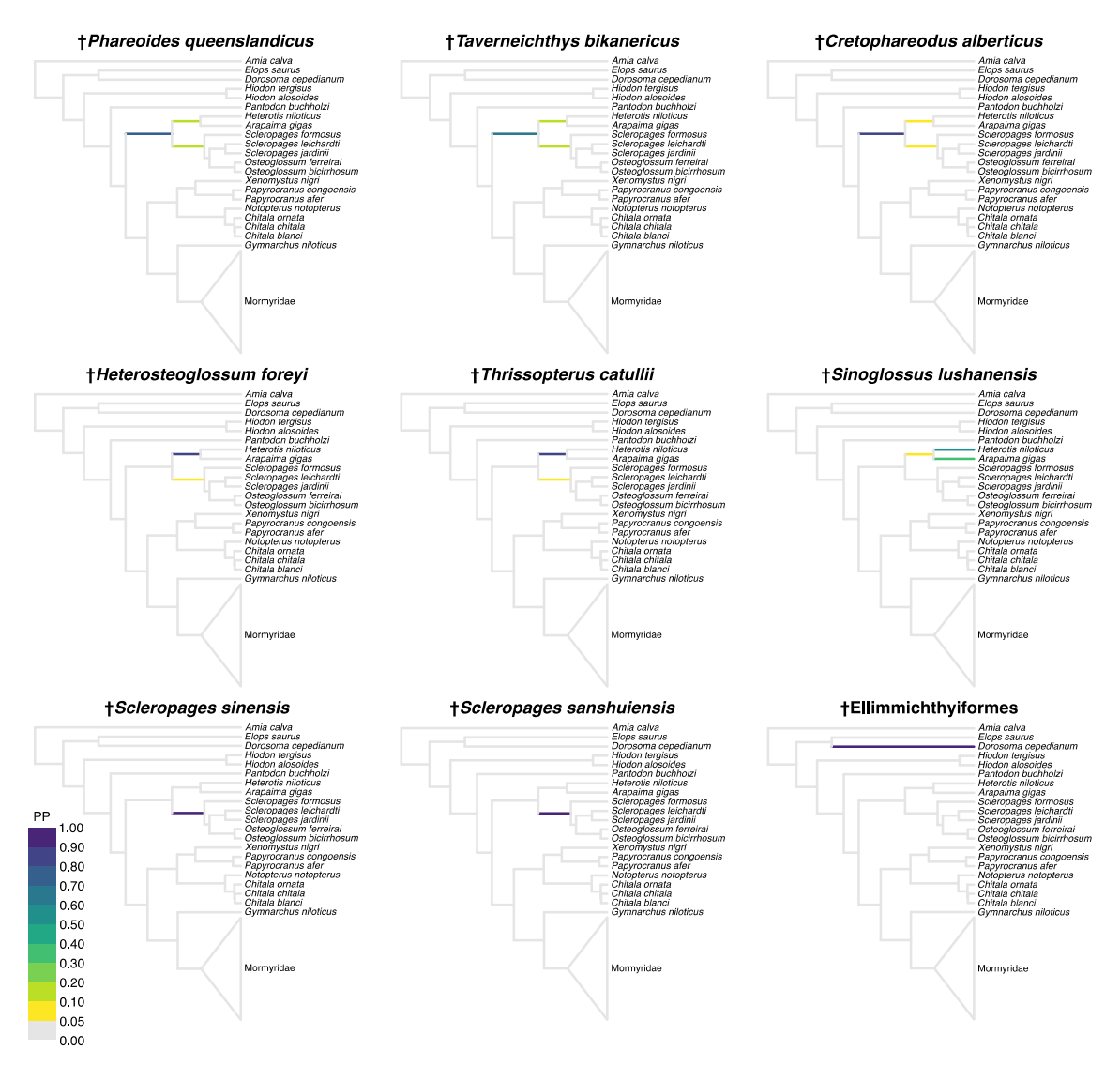


Figure S2 (*part three*). Phylogenetic position of extinct taxa in respect to extant ones across the Bayesian posterior distribution of time-calibrated trees. Mormyrid species were collapsed for clarity, as no fossil was ever reconstructed to fall within crown Mormyridae. PP = posterior probability.

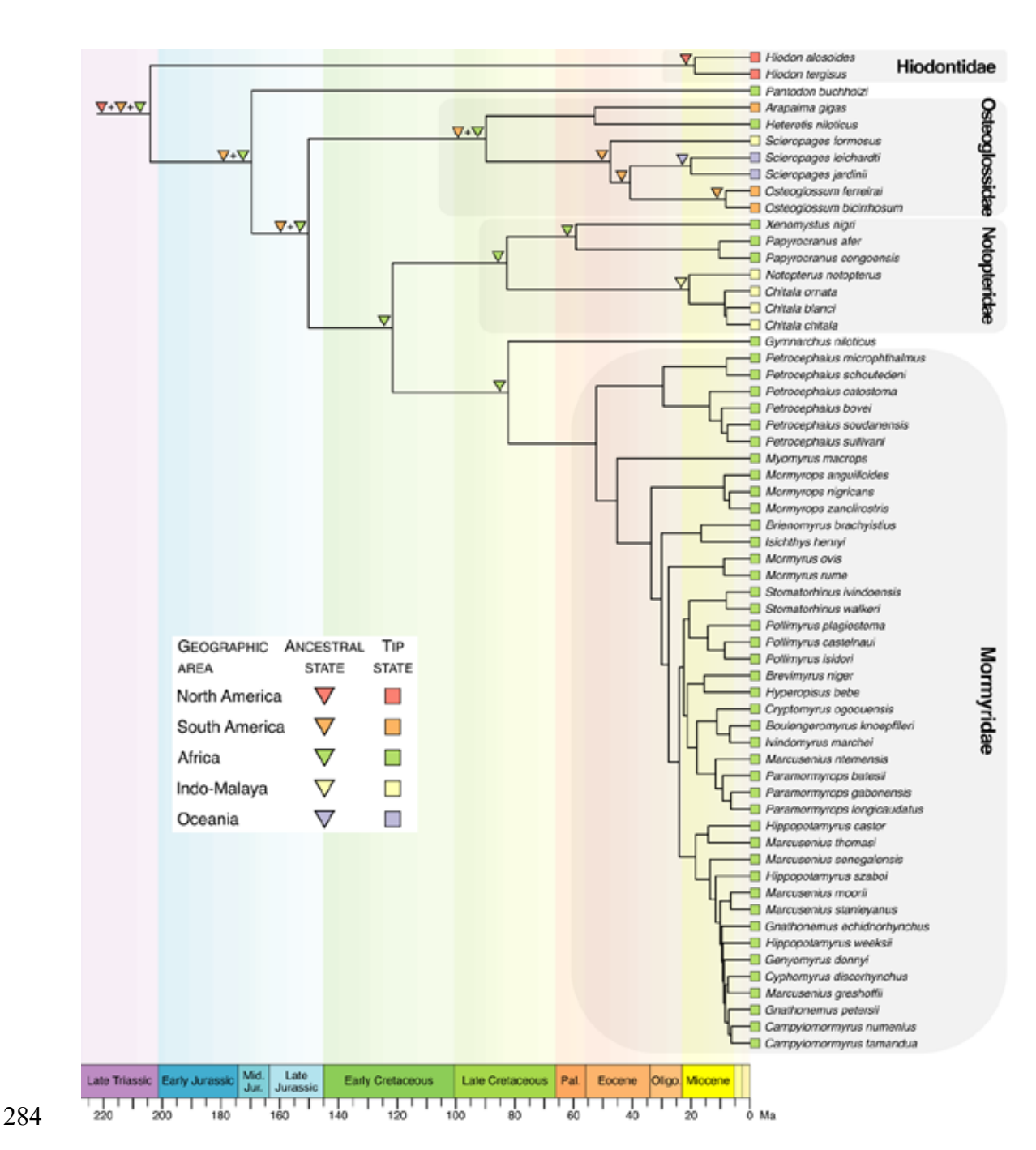


Figure S3. Biogeographic history of Osteoglossomorpha when excluding extinct taxa. The phylogeny plotted here is the 'AllCompat' summary consensus tree from the Bayesian total-evidence analysis, with extinct taxa pruned out. Tips are colored according to geographic distribution. Colored triangles at internal nodes represent the most likely ancestral geographic area under the DEC+*j* model when it is at least 3.2 times more likely than the second-most likely geographic area, indicating substantial strength of evidence under a Bayes factor framework. Colored triangles at internal nodes for which all descendant tips and the immediately ancestral node inhabit the same area were masked to avoid figure cluttering. Highlighted clades refer to crown groups. Ma = million years ago.

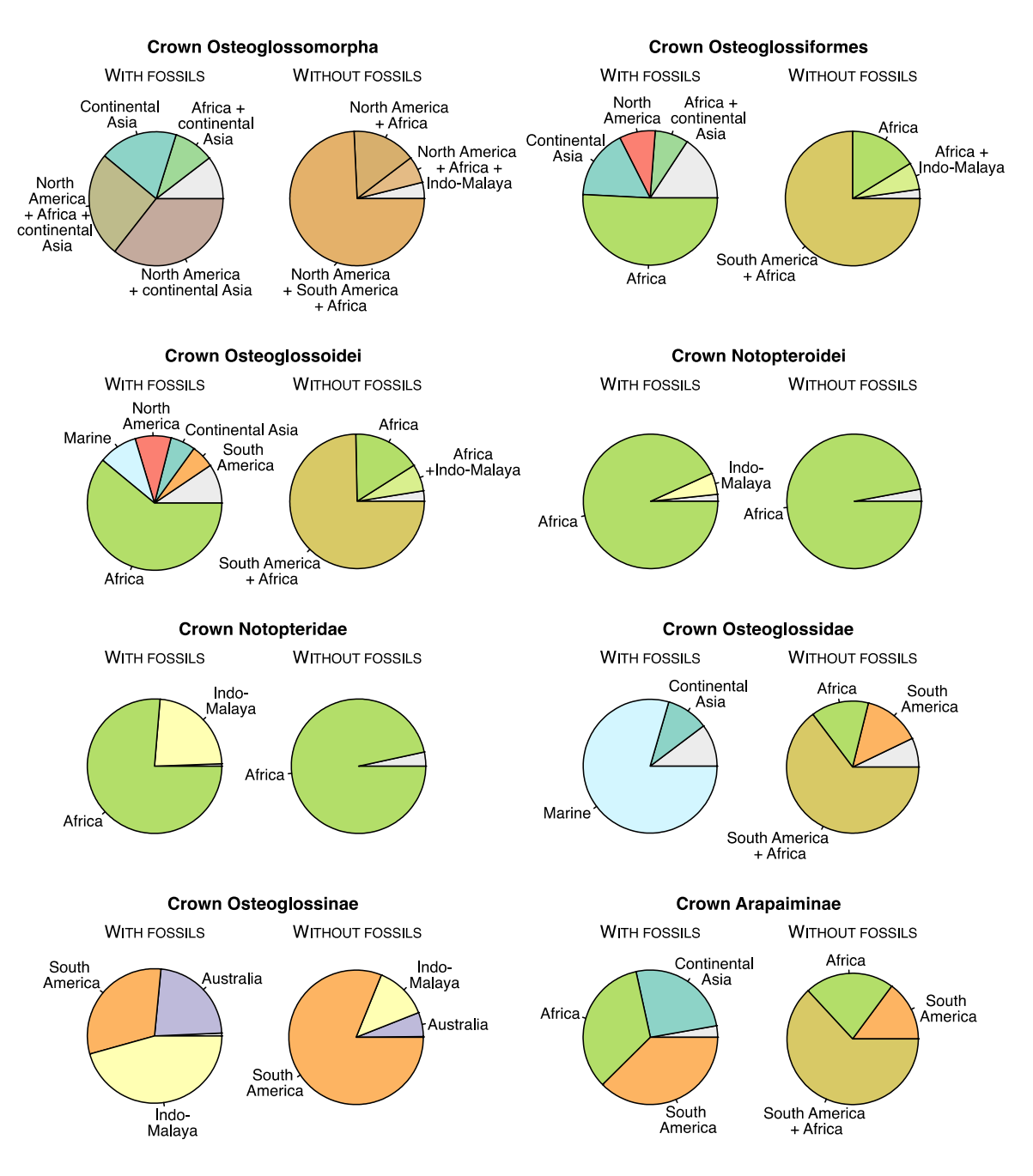


Figure S4. Marginal probabilities of ancestral biogeographic areas under the DEC+*j* model for selected clades when fossils are included in (*left*) or excluded from the analysis (*right*). Probabilities of areas with fossils included are integrated over phylogenetic uncertainty (that is, integrated over a random sample of 200 phylogenies from the Bayesian posterior distribution). Areas with probability <0.05 are collapsed together into the gray slice of the pie chart.

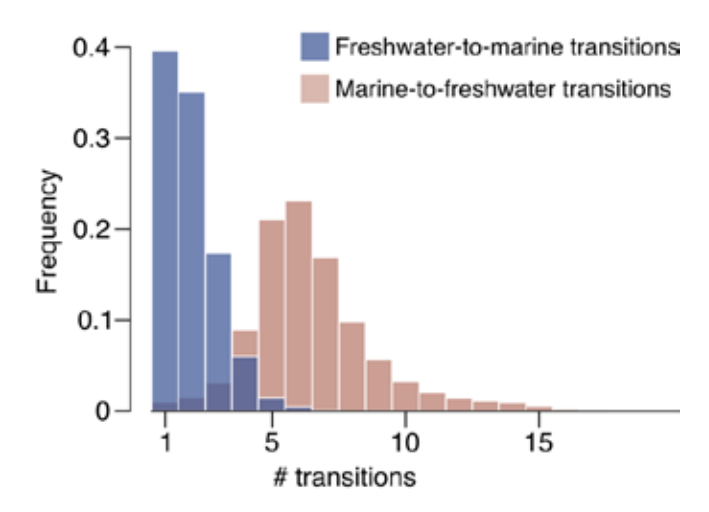


Figure S5. Distribution of the inferred number of environmental transitions in Osteoglossomorpha under an all-rates-different (ARD) model when accounting for phylogenetic uncertainty. Transitions were tabulated across a random sample of 1000 phylogenies from the Bayesian posterior distribution, with 10 stochastic character mappings generated for each phylogeny. Freshwater-to-marine transitions are in dark blue, marine-to-freshwater transitions are in brown.

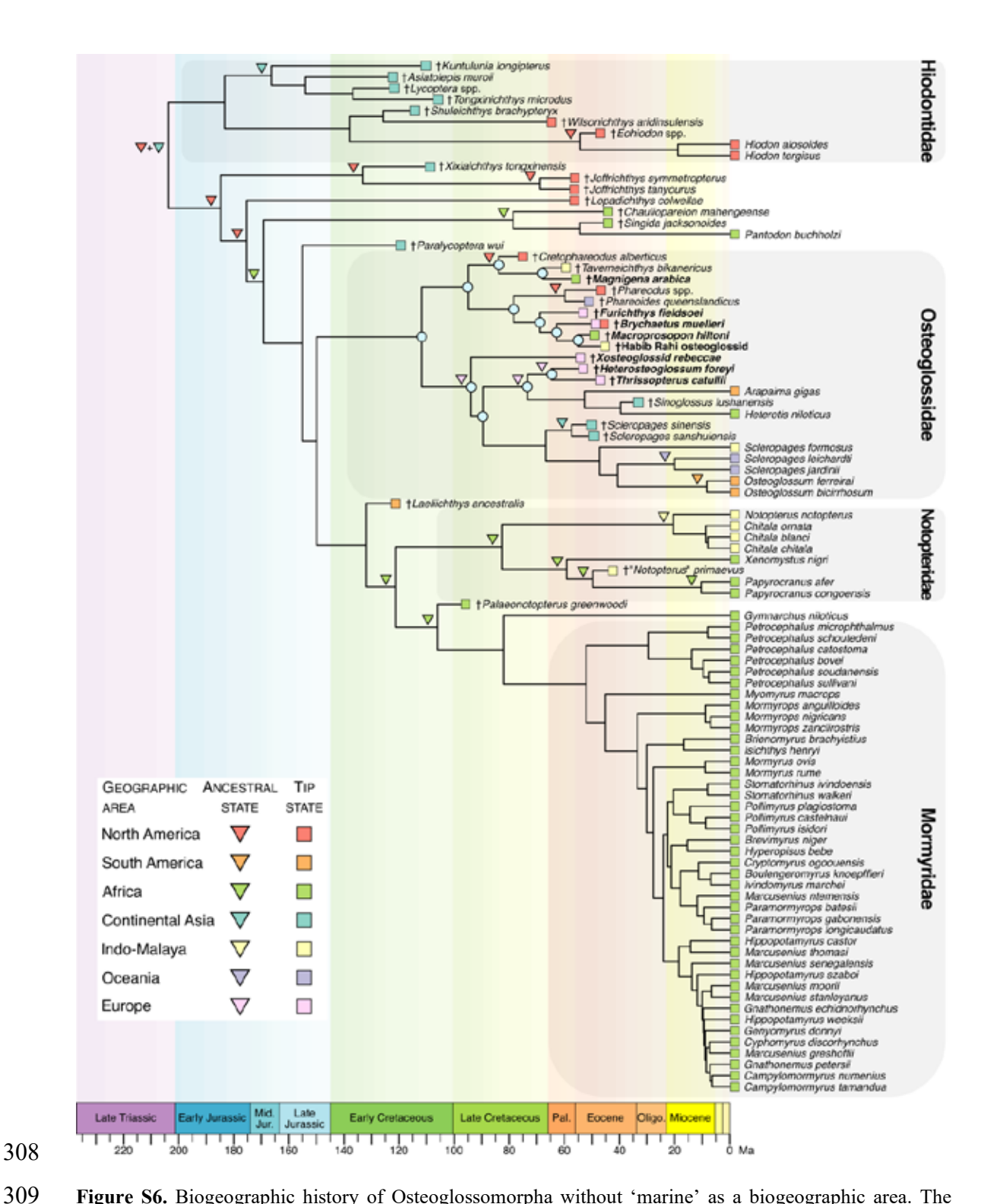


Figure S6. Biogeographic history of Osteoglossomorpha without 'marine' as a biogeographic area. The phylogeny plotted here is the 'AllCompat' summary consensus tree from the Bayesian total-evidence analysis. Tips are colored according to geographic distribution. Blue circles at internal nodes indicate nodes reconstructed as marine in the ancestral habitat estimation (Fig. 4). Colored triangles at internal nodes represent the most likely ancestral geographic area under the DEC+*j* model when it is at least 3.2 times more likely than the second-most likely geographic area, indicating substantial strength of evidence under a Bayes factor framework. Colored triangles at internal nodes for which all descendant tips and the immediately

ancestral node inhabit the same area were masked to avoid figure cluttering. Highlighted clades refer to crown groups. Ma = million years ago.

Partition	Partition content
1	12S rRNA, 16S rRNA, 1st codon position of cytb
2	1st codon position of <i>coI</i>
3	2nd codon position of <i>col</i> and <i>cytb</i>
4	3rd codon position of <i>coI</i>
5	3rd codon position of <i>cytb</i>
6	1st codon position of rag1, rag2, glyt, ficd, megf8, pdzd8, suox and vcpip1
7	2nd codon position of rag1, rag2, glyt, ficd, megf8, pdzd8, suox and vcpip1
8	3rd codon position of rag1, rag2, glyt, ficd, megf8, pdzd8, suox and vcpip1

Table S1. Molecular dataset partitions, as determined by PartitionFinder 2 [41].

Operational Taxonomic Unit (OTU)	Min_age	Max_age	References	
†Ellimmichthyiformes	40.4	133.9	42,43,44	
†Asiatolepis muroii	119.1	129.4	16	
†Brychaetus muelleri	49	52	45	
†Chauliopareion mahengeense	45.7	46.3	46,47	
†Cretophareodus alberticus	76	78	14,48	
†Eohiodon spp.	46.2	51.6	32,49,50	
†Furichthys fieldsoei	54	56	5,51	
Habib Rahi osteoglossid	46	48	52	
†Heterosteoglossum foreyi	54	56	5,51	
†Joffrichthys symmetropterus	56	60.2	53,54	
†Joffrichthys tanyourus	56	60.2	53,54	
†Kuntulunia longipterus	100.5	121.4	15	
†Laeliichthys ancestralis	121.4	125	55	
†Lopadichthys colwellae	56	60.2	53,54	
† <i>Lycoptera</i> spp.	119.1	129.4	56	
†Macroprosopon hiltoni	47.8	56	1	
†Magnigena arabica	56	59.2	18	
†Notopterus primaevus	37.7	56	57,58	
†Palaeonotopterus greenwoodi	95	100.5	59	
†Paralycoptera wui	113	129.4	60	
†Phareodus spp.	45.5	51.6	27,49,61	
†Phareoides queenslandicus	45	59.2	7,62	
†Scleropages sanshuiensis	47.8	56	13	
†Scleropages sinensis	47.8	56	12	
†Shuleichthys brachypteryx	112.5	120.5	63	
†Singida jacksonoides	45.7	46.3	46,47	
†Sinoglossus lushanensis	23	37.7	64,65	
†Taverneichthys bikanericus	56	66	9	
†Thrissopterus catullii	48.5	49	11,66	

†Tongxinichthys microdus	100.5	113	17
†Wilsonichthys aridinsulensis	66	67.1	67
†Xixiaichthys tongxinensis	108	113.5	68,69
†Xosteoglossid rebeccae	55.5	56.5	5,51

Table S2. Minimum and maximum ages (in million years ago) assigned to fossil tips for the total-evidence phylogenetic analysis.

Operational Taxonomic Unit (OTU)	Paleoenvironment	Ecology	References	
†Asiatolepis muroii	Lacustrine	Freshwater	16,70	
†Brychaetus muelleri	Oceanic (continental shelf)	shelf) Marine		
†Chauliopareion mahengeense	Lacustrine	Freshwater	46,47	
†Cretophareodus alberticus	Fluvial (floodplain)	Freshwater	14,48	
†Eohiodon spp.	Lacustrine	Freshwater	32,49	
†Furichthys fieldsoei	Oceanic	Marine	5,51	
Habib Rahi osteoglossid	Oceanic (continental shelf)	Marine	52,71	
†Heterosteoglossum foreyi	Oceanic	Marine	5	
†Joffrichthys symmetropterus	Fluviolacustrine	Freshwater	53,54	
†Joffrichthys tanyourus	Fluviolacustrine	Freshwater	53,54	
†Kuntulunia longipterus	Lacustrine	Freshwater	15,72	
†Laeliichthys ancestralis	Lacustrine	Freshwater	55,73	
†Lopadichthys colwellae	Fluviolacustrine	Freshwater	53,54	
†Lycoptera spp.	Lacustrine	Freshwater	56,70	
†Macroprosopon hiltoni	Shallow marine (epicontinental sea)	Marine	1,74	
†Magnigena arabica	Shallow marine/lagoonal	Marine	18,75	
†Notopterus primaevus	Lacustrine	Freshwater	57,58	
†Palaeonotopterus greenwoodi	Fluvial (floodplain/alluvial cone)	Freshwater	59,76	
†Paralycoptera wui	Fluviolacustrine Fre		60,77	
† <i>Phareodus</i> spp.	Lacustrine	Freshwater	27,49	
†Phareoides queenslandicus	Lacustrine	Freshwater	7,62,78	
†Scleropages sanshuiensis	Lacustrine	Freshwater	13	
†Scleropages sinensis	Lacustrine	Freshwater	12	
†Shuleichthys brachypteryx	Lacustrine	Freshwater	63	
†Singida jacksonoides	Lacustrine	Freshwater	46,47	
†Sinoglossus lushanensis	Fluviolacustrine	Freshwater		
†Taverneichthys bikanericus	Deltaic (?)	Freshwater	9	
†Thrissopterus catullii	Shallow marine (peri-reefal system)	Marine	11,66	
†Tongxinichthys microdus	Lacustrine	Freshwater	17,72	

†Wilsonichthys aridinsulensis	Fluvial (paleochannel)	Freshwater	67
†Xixiaichthys tongxinensis	Lacustrine	Freshwater	68,72
†Xosteoglossid rebeccae	Closed marine basin	Marine	5,51

Table S3. Paleoenvironmental attribution of fossil deposits where extinct osteoglossomorph taxa have been found. The 'Ecology' column indicates the state (freshwater vs marine) assigned to each extinct taxon for the ancestral habitat estimation analysis.

	LnL	numparams	d	e	j	AICc	AICc_wt
DEC	-113.6	2	0.0007	1.0e-12	0	231.3	3.7e-09
DEC+J	-93.16	3	1.0e-12	1.0e-12	0.02	192.6	0.91
DIVALIKE	-211	2.	0.01	0.01	0	426	1.8e-51
DIVILIKE	211	_	0.01	0.01	O	120	1.00 31
DIVALIKE+J	-211	3	0.01	0.01	0.0001	428.3	5.8e-52
BAYAREALIKE	-228.2	2	0.01	0.01	0	460.5	6.1e-59
BAYAREALIKE+J	-95.48	3	1.0e-12	1.0e-12	0.021	197.2	0.089

Table S4. Model comparison between biogeographic models in BioGeoBEARS, using the 'AllCompat' summary consensus tree obtained from the total-evidence phylogenetic analysis. LnL = log-transformed likelihood; numparams = number of free parameters; d = dispersal (range expansion) rate parameter; e = extinction/extirpation rate parameter; j = jump dispersal rate parameter; AlCc = Akaike Information Criterion corrected for sample size; AlCc_wt = Akaike weights for Akaike Information Criterion corrected for sample size.

References

- 1. A. Capobianco, S. Zouhri, M. Friedman, A long-snouted marine bonytongue (Teleostei: Osteoglossidae) from the early Eocene of Morocco and the phylogenetic affinities of marine osteoglossids. *Zool. J. Linn. Soc.* (in press).
- 2. L. Taverne, Osteologie, phylogénèse et systématique des Téléostéens fossiles et actuels de super-ordre des Ostéoglossomorphes. Deuxième partie. Ostéologie des genres *Phareodus*, *Phareoides*, *Brychaetus*, *Musperia*, *Pantodon*, *Singida*, *Notopterus*, *Xenomystus* et *Papyrocranus*. *Académie Royale de Belgique*, *Mémoires de la Classe des Sciences*, *Collection in-8° 2e série 42*, 1–213 (1978).
- 3. E. J. Hilton, Comparative osteology and phylogenetic systematics of fossil and living bony-tongue fishes (Actinopterygii, Teleostei, Osteoglossomorpha). *Zool. J. Linn. Soc.* **137**, 1–100 (2003).
- 4. L. Taverne, Ostéologie des genres Mormyrus Linné, Mormyrops Müller, Hyperopisus Gill, Isichthys Gill, Myomyrus Boulenger, Stomatorhinus Boulenger et Gymnarchus Cuvier: considérations générales sur la systématique des poissons de l'ordre des Mormyriformes. Musée Royal de l'Afrique centrale—Tervuren, Belgique Annales—Serie in-8°—Sciences Zoologiques 200, 1–198 (1972).
- 5. N. Bonde, Osteoglossomorphs of the marine Lower Eocene of Denmark-with remarks on other Eocene taxa and their importance for palaeobiogeography. *Geol. Soc. Spec. Publ.* **295**, 253–310 (2008).

- E. S. Hills, Tertiary fresh water fishes from southern Queensland. *Mem. Queensl. Mus.* 10, 157–174
 (1934).
- 7. G.-Q. Li, Systematic position of the Australian fossil osteoglossid fish †*Phareodus* (= *Phareoides*) queenslandicus Hills. *Mem. Queensl. Mus.* **37**, 287–300 (1994).
- 360 8. L. Taverne, New insights on the osteology and taxonomy of the osteoglossid fishes *Phareodus*,
 361 Brychaetus and Musperia (Teleostei, Osteoglossomorpha). Bulletin de l'Institut Royal des Sciences
 362 Naturelles de Belgique, Sciences de la Terre 79, 175–190 (2009).
- K. Kumar, R. S. Rana, B. S. Paliwal, Osteoglossid and lepisosteid fish remains from the Paleocene
 Palana Formation, Rajasthan, India. *Palaeontol.* 48, 1187–1210 (2005).
- L. Taverne, K. Kumar, R. S. Rana, Complement to the study of the Indian Paleocene osteoglossid
 fish genus *Taverneichthys* (Teleostei, Osteoglossomorpha). *Bulletin de l'Institut Royal des Sciences Naturelles de Belgique, Sciences de la Terre* 79, 155–160 (2009).

369

370

- 11. L. Taverne, Les ostéoglossomorphes marins de l'Éocène du Monte Bolca (Italie): *Monopteros* Volta 1796, *Thrissopterus* Heckel, 1856 et *Foreyichthys* Taverne, 1979. Considérations sur la phylogénie des téléostéens ostéoglossomorphes. *Studi e Ricerche sui Giacimenti Terziari di Bolca, VII Miscellanea Paleontologica* **4**, 67–158 (1998).
- 372 12. J.-Y. Zhang, M. V. H. Wilson, First complete fossil *Scleropages* (Osteoglossomorpha). *Vertebrata* 373 *PalAsiatica* **55**, 1–23 (2017).
- 374 13. J.-Y. Zhang, A new species of *Scleropages* (Osteoglossidae, Osteoglossomorpha) from the Eocene of Guangdong, China. *Vertebrata PalAsiatica* **58**, 100–199 (2020).
- 376
 14. G.-Q. Li, "A new species of Late Cretaceous osteoglossid (Teleostei) from the Oldman Formation

 377
 of Alberta, Canada, and its phylogenetic relationships" in *Mesozoic Fishes. Systematics and Paleoecology*, G. Arratia, G. Viohl, Eds. (Verlag Dr. F. Pfeil, München, 1996), pp. 285–298.
- 379 15. J.-Y. Zhang, Morphology and phylogenetic relationships of †*Kuntulunia* (Teleostei: 380 Osteoglossomorpha). *J. Vertebr. Paleontol.* **18**, 280–300 (1998).
- 381 16. J.-Y. Zhang, "Validity of the osteoglossomorph genus † *Asiatolepis* and a revision of † *Asiatolepis*382 muroii († *Lycoptera muroii*)" in *Origin and Phylogenetic Interrelationships of Teleosts*, J. S. Nelson,
 383 H.-P. Schultze, M. V. H. Wilson, Eds. (Verlag Dr. F. Pfeil, München, 2010), pp. 239–249.
- J.-Y. Zhang, F. Jin, "A revision of † Tongxinichthys Ma 1980 (Teleostei: Osteoglossomorpha) from
 the Lower Cretaceous of northern China" in Mesozoic Fishes 2 Systematics and Fossil Record, G.
 Arratia, H.-P. Schultze, Eds. (Verlag Dr. F. Pfeil, München, 1999), pp. 385–396.
- 387 18. P. L. Forey, E. J. Hilton, "Two new tertiary osteoglossid fishes (Teleostei: Osteoglossomorpha) with
 388 notes on the history of the family" in *Morphology, Phylogeny and Paleobiogeography of Fossil*389 *Fishes*, D. K. Elliott, J. G. Maisey, X. Yu, D. Miao, Eds. (Verlag Dr. F. Pfeil, München, 2010), pp.
 390 215–246.
- 391 19. R. D. Peterson *et al.*, Phylogenomics of bony-tongue fishes (Osteoglossomorpha) shed light on the craniofacial evolution and biogeography of the weakly electric clade (Mormyridae). *Syst. Biol.* **71**,

- 393 1032–1044 (2022).
- 20. D. Eme, M. J. Anderson, C. D. Struthers, C. D. Roberts, L. Liggins, An integrated pathway for building regional phylogenies for ecological studies. *Glob. Ecol. Biogeogr.* **28**, 1899–1911 (2019).
- R. Froese, D. Pauly, Eds. FishBase. World Wide Web electronic publication, version (10/2020).
 Available at www.fishbase.org
- 398 22. K. Katoh, D. M. Standley, MAFFT multiple sequence alignment software version 7: improvements in performance and usability. *Mol. Biol. Evol.* **30**, 772–780 (2013).
- 400 23. R. C. Edgar, MUSCLE: multiple sequence alignment with high accuracy and high throughput.

 401 Nucleic Acids Res. 32, 1792–1797 (2004).
- 402 24. T. Lassmann, E. L. Sonnhammer, Automatic assessment of alignment quality. *Nucleic Acids Res.* 403 33, 7120–7128 (2005).
- 404 25. J. Castresana, Selection of conserved blocks from multiple alignments for their use in phylogenetic analysis. *Mol. Biol. Evol.* 17, 540–552 (2000).
- 406 26. A. Larsson, AliView: a fast and lightweight alignment viewer and editor for large datasets.

 407 *Bioinformatics* **30**, 3276–3278 (2014).
- 408 27. G.-Q. Li, L. Grande, M. V. H. Wilson, The species of †*Phareodus* (Teleostei: Osteoglossidae) from the Eocene of North America and their phylogenetic relationships. *J. Vertebr. Paleontol.* 17, 487–410 505 (1997).
- 411 28. H. F. Roellig, The cranial osteology of *Brychaetus muelleri* (Pisces Osteoglossidae) Eocene, Isle of Sheppey. *J. Paleontol.* **48**, 947–951 (1974).
- 413 29. W. G. Ridewood, On the cranial osteology of the fishes of the families Mormyridae, Notopteridae and Hyodontidae. *Zool. J. Linn. Soc.* **29**, 188–217 (1904).
- 30. L. Taverne, Ostéologie, phylogénèse et systématique des Téléostéens fossiles et actuels du superordre des Ostéoglossomorphes, Première partie. Ostéologie des genres *Hiodon*, *Eohiodon*, *Lycoptera*, *Osteoglossum*, *Scleropages*, *Heterotis* et *Arapaima*. *Académie Royale de Belgique*, *Mémoires de la Classe des Sciences*, *Collection in-8° – 2e série* **42**, 1–235 (1977).
- 419 31. E. J. Hilton, R. Britz, "The caudal skeleton of osteoglossomorph fishes, revisited: comparisons, homologies, and characters" in *Origin and phylogenetic interrelationships of Teleosts*, J. S. Nelson, 421 H. P. Schultze, M. V. H. Wilson, Eds. (Verlag Dr. F. Pfeil, München, 2010), pp. 219–237.
- 32. E. J. Hilton, L. Grande, Fossil mooneyes (Teleostei: Hiodontiformes, Hiodontidae) from the Eocene
 of western North America, with a reassessment of their taxonomy. *Geol. Soc. Spec. Publ.* 295, 221–
 251 (2008).
- 425 33. M. V. H. Wilson, A. M. Murray, Osteoglossomorpha: phylogeny, biogeography, and fossil record and the significance of key African and Chinese fossil taxa. *Geol. Soc. Spec. Publ.* **295**, 185–219 (2008).

- 428 34. S. Lavoué, Was Gondwanan breakup the cause of the intercontinental distribution of Osteoglossiformes? A time-calibrated phylogenetic test combining molecular, morphological, and paleontological evidence. *Mol. Phylogenet. Evol.* **99**, 34–43 (2016).
- 431 35. P. L. Forey, A Cretaceous notopterid (Pisces: Osteoglossomorpha) from Morocco. *S. Afr. J. Sci.* **93**, 432 564–569 (1997).
- 433 36. L. Taverne, J. G. Maisey, A notopterid skull (Teleostei, Osteoglossomorpha) from the continental early Cretaceous of southern Morocco. *Am. Mus. Novit.* **3260**, 1–12 (1999).
- 37. J. G. Inoue, Y. Kumazawa, M. Miya, M. Nishida, The historical biogeography of the freshwater knifefishes using mitogenomic approaches: a Mesozoic origin of the Asian notopterids (Actinopterygii: Osteoglossomorpha). *Mol. Phylogenet. Evol.* **51**, 486–499 (2009).
- 438 38. E. J. Hilton, S. Lavoué, A review of the systematic biology of fossil and living bonytongue fishes, 439 Osteoglossomorpha (Actinopterygii: Teleostei). *Neotrop. Ichthyol.* **16**, e180031 (2018).
- 39. A. Capobianco, M. Friedman, Vicariance and dispersal in southern hemisphere freshwater fish clades: a palaeontological perspective. *Biol. Rev.* **94**, 662–699 (2019).
- 442 40. P. Bănărescu, Zoogeography of Fresh Waters. Vol. 2 (AULA-Verlag, Wiesbaden, 1991).
- 41. R. Lanfear, P. B. Frandsen, A. M. Wright, T. Senfeld, B. Calcott, PartitionFinder 2: new methods for selecting partitioned models of evolution for molecular and morphological phylogenetic analyses. *Mol. Biol. Evol.* **34**, 772–773 (2017).
- 42. F. J. Poyato-Ariza, M. A. López-Horgue, F. García-Garmilla, A new early Cretaceous clupeomorph fish from the Arratia Valley, Basque Country, Spain. *Cretac. Res.* **21**, 571–585 (2000).
- 43. M.-M. Chang, J. G. Maisey, Redescription of †*Ellimma branneri* and †*Diplomystus shengliensis*, and relationships of some basal clupeomorphs. *Am. Mus. Novit.* **2003**, 1–35 (2003).
- 450 44. G. Marramà, A. F. Bannikov, J. Kriwet, G. Carnevale, An Eocene paraclupeid fish (Teleostei, Ellimmichthyiformes) from Bolca, Italy: the youngest marine record of double-armoured herrings.

 452 *Pap. Palaeontol.* 5, 83–98 (2019).
- 45. M. Friedman, H. T. Beckett, R. A. Close, Z. Johanson, The English chalk and London clay: two remarkable British bony fish Lagerstätten. *Geol. Soc. Spec. Publ.* **430**, 165–200 (2016).
- 455 46. T. Harrison *et al.*, "Paleontological investigations at the Eocene locality of Mahenge in north-central Tanzania, East Africa" in *Eocene biodiversity: unusual occurrences and rarely sampled habitats*, 457 G. F. Gunnell, Ed. (Springer, New York, 2001), pp. 39–74.
- 458 47. A. M. Murray, M. V. H. Wilson, Description of a new Eocene osteoglossid fish and additional information on †Singida jacksonoides Greenwood and Patterson, 1967 (Osteoglossomorpha), with an assessment of their phylogenetic relationships. Zool. J. Linn. Soc. 144, 213–228 (2005).
- 48. D. A. Eberth *et al.*, Calibrating geologic strata, dinosaurs, and other fossils at Dinosaur Provincial Park (Alberta, Canada) using a new CA-ID-TIMS U–Pb geochronology. *Can. J. Earth Sci.* e-First, 20 pp. (2023).

- 464 49. M. E. Smith, K. R. Chamberlain, B. S. Singer, A. R. Carroll, Eocene clocks agree: Coeval 465 40Ar/39Ar, U-Pb, and astronomical ages from the Green River Formation. *Geology* **38**, 527–530 (2010).
- 50. G. E. Mustoe, Cyclic sedimentation in the Eocene Allenby Formation of south-central British Columbia and the origin of the Princeton Chert fossil beds. *Can. J. Earth Sci.* **48**, 25–43 (2011).
- 51. E. W. Stokke, E. J. Liu, M. T. Jones, Evidence of explosive hydromagmatic eruptions during the emplacement of the North Atlantic Igneous Province. *Volcanica* 3, 227–250 (2020).
- 52. P. D. Gingerich, Stratigraphic and micropaleontological constraints on the middle Eocene age of the mammal-bearing Kuldana Formation of Pakistan. *J. Vertebr. Paleontol.* **23**, 643–651 (2003).
- 53. G. L. Hoffman, R. A. Stockey, Geological setting and paleobotany of the Joffre Bridge Roadcut fossil locality (Late Paleocene), Red Deer Valley, Alberta. *Can. J. Earth Sci.* **36**, 2073–2084 (1999).
- A. M. Murray, D. K. Zelenitsky, D. B. Brinkman, A. G. Neuman, Two new Palaeocene osteoglossomorphs from Canada, with a reassessment of the relationships of the genus † *Joffrichthys*, and analysis of diversity from articulated versus microfossil material. *Zool. J. Linn. Soc.* 183, 907–944 (2018).
- 55. P. M. Brito, F. J. Figueiredo, M. E. C. Leal, A revision of *Laeliichthys ancestralis* Santos, 1985 (Teleostei: Osteoglossomorpha) from the Lower Cretaceous of Brazil: Phylogenetic relationships and biogeographical implications. *PLoS One* **15**, e0241009 (2020).
- 482 56. F. Jin, J. Zhang, Z. Zhou, Late Mesozoic fish fauna from western Liaoning, China. *Vertebrata*483 *PalAsiatica* 33, 169–193 (1995).
- 484 57. M. Sanders, Die Fossilen Fische der Alttertiären Süsswasserablagerungen aus Mittel-Sumatra.

 485 Verhandelingen van het Geologisch-Mijnbouwkundig Genootschap voor Nederland en Koloni'n

 486 Geologische Series 11, 1–144 (1934).
- 58. A. M. Murray, Early Cenozoic cyprinoids (Ostariophysi: Cypriniformes: Cyprinidae and Danionidae) from Sumatra, Indonesia. *J. Vertebr. Paleontol.* **40**, e1762627 (2020).
- 59. L. Cavin *et al.*, Taxonomic composition and trophic structure of the continental bony fish assemblage from the early Late Cretaceous of southeastern Morocco. *PLoS One* **10**, e0125786 (2015).
- 492 60. G. H. Xu, M. Chang, Redescription of †*Paralycoptera wui* Chang. & Chou, 1977 (Teleostei: 493 Osteoglossoidei) from the Early Cretaceous of eastern China. *Zool. J. Linn. Soc.* **157**, 83–106 (2009).
- 495
 61. P. C. Murphey, E. Evanoff, "Paleontology and stratigraphy of the middle Eocene Bridger Formation,
 496 southern Green River basin, Wyoming" in *Proceedings of the 9th Conference on Fossil Resources*,
 497 pp. 83–109 (2011).
- 498 62. D. C. Green, N. C. Stevens, Age and stratigraphy of Tertiary volcanics and sedimentary rocks of the Ipswich district, southeast Queensland. *Queensland Government Mining Journal* **76**, 148–150 (1975).

- 501 63. A. M. Murray, H. L. You, C. Peng, A new Cretaceous osteoglossomorph fish from Gansu Province, China. *J. Vertebr. Paleontol.* **30**, 322–332 (2010).
- 503 64. D. Z. Su, The discovery of a fossil osteoglossid fish in China. *Vertebrata PalAsiatica* **24**, 10 (1986).
- 504 65. H. Huang, D. He, D. Li, Y. Li, Detrital zircon U-Pb ages of Paleogene deposits in the southwestern Sichuan foreland basin, China: Constraints on basin-mountain evolution along the southeastern margin of the Tibetan Plateau. *GSA Bulletin* 132, 668–686 (2020).
- 507 66. M. Friedman, G. Carnevale, The Bolca Lagerstätten: shallow marine life in the Eocene. *J. Geol.* 508 *Soc. London* 175, 569–579 (2018).
- A. M. Murray, M. G. Newbrey, A. G. Neuman, D. B. Brinkman, New articulated osteoglossomorph
 from Late Cretaceous freshwater deposits (Maastrichtian, Scollard Formation) of Alberta, Canada.
 J. Vertebr. Paleontol. 36, e1120737 (2016).
- 512 68. J.-Y. Zhang, New fossil osteoglossomorph from Ningxia, China. *J. Vertebr. Paleontol.* **24**, 515–524 (2004).
- 514 69. M. Zhang, S. Dai, B. Du, L. Ji, S. Hu, Mid-Cretaceous hothouse climate and the expansion of early angiosperms. *Acta Geologica Sinica* **92**, 2004–2025 (2018).
- 516 70. B. Jiang, G. E. Harlow, K. Wohletz, Z. Zhou, J. Meng, New evidence suggests pyroclastic flows are responsible for the remarkable preservation of the Jehol biota. *Nat. Commun.*, **5**, 3151 (2014).
- 518 71. U. Khitab, M. Umar, M. Jamil, Microfacies, diagenesis and hydrocarbon potential of Eocene carbonate strata in Pakistan. *Carbonates Evaporites*, **35**, 70 (2020).
- Y. Ma, J. Pan, D. Fu, Y. Wang, Y. Wang, D. Chang, L. Cheng, W. Fu, The organic geochemistry,
 pore structure and methane adsorption/storage capacity of lacustrine shales from the Cretaceous
 Madongshan Formation, Liupanshan Basin, China. J. Nat. Gas Sci. Eng., 96, 104287 (2021).

524

525

- 73. A. M. Leite, D. A. Do Carmo, L. R. Gonçalves, D. Xi, Biostratigraphy of Liminic Ostracoda (Crustacea) from the Quiricó Formation, Lower Cretaceous of the São Francisco Basin, Minas Gerais State, Brazil: An approach on paleozoogeographic evolution of Gondwana. Cretac. Res., 158, 105816 (2024).
- J. Yans, M. B. Amaghzaz, B. Bouya, H. Cappetta, P. Iacumin, L. Kocsis, M. Mouflih, O. Selloum,
 S. Sen, J.-Y. Storme, E. Gheerbrant, First carbon isotope chemostratigraphy of the Ouled Abdoun
 phosphate Basin, Morocco; implications for dating and evolution of earliest African placental
 mammals. Gondwana Res., 25, 257–269 (2014).
- 531 75. A.J. AlTammar, Stratigraphy of The Central Red Sea Margin: New Insights on the Tectono-532 stratigraphy of the Pre-and Syn-rift sedimentary sections and Arabian Plateau Uplift (M. Sc. thesis) 533 (2021).
- 534 76. I. El Konty, A. Algouti, A. Algouti, A. Farah, A. Aboulfaraj, F. Hadach, Contribution to the sedimentological, paleo environmental and paleogeographical study of Infra-Cenomanian sediments from the South Slope of the Central High Atlas (Morocco). *Geopersia*, **12**, 265–285 (2022).

538	77. Z. Jiang, H. Wu, N. Tian, Y. Wang, A. Xie, A new species of conifer wood Brachyoxylon from the
539	Cretaceous of Eastern China and its paleoclimate significance. Hist. Biol., 33, 1989–1995 (2021).
540	78. A. Rix, Coal, bees and fossils: The history and significance of the Redbank Plains Formation fossil
541	sites, South East Queensland. The Proceedings of the Royal Society of Queensland, 131, 131-144
542	(2022).
543	
544	